BIOTURBATION-INFLUENCED FLUID PATHWAYS WITHIN A CARBONATE PLATFORM SYSTEM: THE LOWER CRETACEOUS (APTIAN–ALBIAN) GLEN ROSE LIMESTONE

JAMES A. GOLAB[a,*], JON J. SMITH[b], ALLAN K. CLARK[c],AND ROBERT R. MORRIS[c]

[a]*Department of Geology, University of Kansas, 1475 Jayhawk Blvd., rm 120, Lindley Hall, Lawrence, Kansas, 66045, USA, [*]jgolab@ku.edu;*

[b]*Kansas Geological Survey, University of Kansas, 1930 Constant Blvd., Lawrence, Kansas, 66046, USA;*

[c]*Texas Water Science Center, U.S. Geological Survey, 5563 De Zavala Rd., Suite 290, San Antonio, Texas, 78249, USA.*

[*]*Corresponding Author*

ABSTRACT

The Aptian–AlbianGlen Rose Limestone (GRL) is an argillaceous shallow-marine carbonate deposit on the Central Texas Platform and contains the upper Trinity aquifer and the upper part of the middle Trinity aquifer. The GRL is divided into Upper and Lower GRL members, which have beenfurther subdivided into hydrostratigraphic units (HSUs). This study uses an integrated ichnological and sedimentological approach to record changes in ichnofabric index (ii) as a proxy for bioturbation within the GRL and relates these changes to fluid flow. Fluid pathways within HSUs are controlled by the complex interaction of faults and fractures, karst development, and large-scale bioturbation-influencedporosity and permeability. The effect of bioturbation-influencedporosity as an aquifer characteristic is the least studied of these factors. Postdepositional solution enhancement of ichnofossils is also common and has increased lateral and vertical fluid connectivity in some HSUs. Most GRL strata are dominated by *Thalassinoides* networks, but also contain *Palaeophycus*, *Planolites*, *Ophiomorpha*, Serpulid worm tubes, rhizoliths, and*Cruziana*.*Thalassinoides* are commonly filled with coarser sediment than the surrounding matrix and act as fluid conduits within an otherwise low permeability matrix. Beds with ii3–4 and burrows with permeable fill transmit water readily. Beds with ii5–6 are commonly muddy and heavily homogenized, restricting fluid flow. Grainstone beds commonly have ii1–2 and are well cemented, restricting fluid flow to low intergranular flow. Pore systems dominated by *Thalassinoides* ichnofabrics, such as the GRL, are difficult to characterize on a large scale using many laboratory methods because they create heterogeneous flow paths depending on difference in permeability between the matrix and burrow fill. Understanding the effects of bioturbation-influenced porosity and permeability on subsurface fluid pathways is vital for creating a geologic and hydrostratigraphic framework for the Trinity aquifer.

Keywords: Trace Fossils; Ichnology; Karst; Hydrostratigraphy; *Thalassinoides*

1.0 Introduction

The Lower Cretaceous (Aptian–Albian) Glen Rose Limestone (GRL) forms the upper Trinity aquifer and the upper part of the middle Trinity aquifer in south-central Texas (TX). The combined Edwards and Trinity aquifer system provides the sole source of freshwater for San Antonio, TX, the seventh largest city in the United States, and the surrounding area (Clark, 2003). It is, therefore, vital to create a robust geologic framework in order to understand the subsurface fluid pathways of the GRL for developmental planning and regulating water usage in south-central TX.

Fluid pathways within the GRL are controlled by the complex interaction of faults and fractures, karst development, and large-scale bioturbation-influenced porosity and permeability (Horvoka et al., 1994). Extensive studies have been conducted on the effects of fracturing (e.g., George, 1952; Maclay and Small, 1976, 1986; Grimshaw and Woodruff, 1986; Maclay 1989; Pantea et al., 2008) and karst (e.g., Horvorka et al, 1994; Maclay, 1995; Scanlon et al., 2003; Faith, 2004; Gary et al., 2013) on Edwards and Trinity aquifer quality; however, few studies have focused on bioturbation-influenced porosity and ichnofabricswithin these systems (i.e., Cunningham and Sukop, 2012).

Ichnofossils are common throughout the carbonate strata of south-central TX and are significant controls on fluid flow. Cunningham and Sukop (2012) showed permeability associated with *Thalassinoides*-dominated ichnofabrics controlled horizontal fluid flow within the overlying Edwards aquifer, where unfilled ichnofossils form interconnected fluid conduits. The mudstone and marl within the GRL; however, complicates such ichnofabric analysis as many GRL *Thalassinoides* are filled with carbonate mudstoneto grainstone acting eitheras barriersor conduitsrespectively. Dissolution of existing ichnofossils is also common in the GRL

and may have increased the vertical and lateral fluid connectivity of some beds. Dissolution of material via meteoric wateralong fluid pathways is a prominent feature in similar carbonate settings (Mylroie and Carew, 1990; Cunningham et al., 2009; Wright et al., 2014) and dissolution of ichnofossils has been shown to increase porosity and permeability in such systems (Cunningham et al., 2009; Tonkin et al., 2010).

This study uses an integrated ichnological and sedimentological approach to record changes in ichnofabric index (ii) as a proxy for bioturbation within the GRL and interprets how these changes relate to subsurface fluid pathways. The GRL is a carbonate platform composed of rudist reefs and subtidalto supratidal facies assigned to the Thalassinoidesichnofacies. The majority of GRL strata are the dominated by coarsening-upward successions of wackestone to packstone with some carbonate mudstone and grainstone. These successions have been interpreted to have been deposited by a tide-dominated system and are commonly muddy with low intergranular permeability. Associated rudist-dominated facies are also muddy, but contain abundant fractures and have high permeability, but limited lateral extent (Petta, 1977). The GRL, therefore,cannot transmit fluid through interparticle porosity easily, but may rely, in part, on bioturbation-influenced porosity (Mathews, 1967; Achauer, 1977; Cunningham and Sukop, 2012; Golab et al., 2015). This biogenic aspect ofkarstic aquifers has generally been overlooked in the literature (Cunningham et al., 2009; Cunningham and Sukop, 2011, 2012; Golab et al., 2015).

2.0 Geological Background

2.1 Depositional and Tectonic History

The GRL is the uppermost formation of the Lower Cretaceous Trinity Group, which is present across most of south-central TX (Fig. 1; von Roemer, 1852; Imlay, 1945). The Trinity Group is a succession of three distinct, second-order,transgressive–regressive sequences composedof a lower siliciclastic lowstand unit and an upper carbonate highstand unit deposited on the shallow-marine Central Texas Platform, which spans from the Llano Uplift southeast to the Stuart City Reef (Fig.1; George, 1952; Winter, 1961; Barnes, 1965; Stricklin et al., 1971; Inden, 1974; Bebout et al., 1977; Barnes, 1981). The three sequences of the Trinity Group in the study area are: 1) the Hosston and Sligo formations; 2) the Hammett Shale and Cow Creek Limestone; and 3) the Hensel Sand and the Glen Rose Limestone(Fig. 2; Stricklin et al., 1971).The Trinity Group is overlain by the Albian Edwards Group, a 120–180 m succession of platform carbonates that accumulated north of the Stuart City Reef across most of central and southern Texas (Fig.1; Rose, 1972). The GRL forms the upper Trinity aquifer and the upper part of the middle Trinity aquifer, which act as a catchment for the Edwards aquifer where it is exposed at the surface (Small and Lambert, 1998; Blome et al., 2007; Clark et al., 2009).

The GRL is an ~120-m-thick succession of argillaceous carbonates with few beds of siliciclastics and is divided into two members: the Upper and Lower GRL (Lazo and Stricklin, 1956; Carew, 1967; Stricklin et al., 1971; Scott et al., 2007). The Lower GRL is ~70-74 m thick within the study area and is characterized by m-scalebeds of mudstone and marls alternating with beds of wackestone to grainstone (Clark, 2003, 2005; Clark and Morris, 2015). These beds are fossiliferous and commonly contain the whole or fragmentary shells of gastropods (e.g., *Nerinea* sp.;*Tylostoma* sp.), bivalves (e.g., *Texigryphea* sp.;*Cucullaea terminalis*), echinoids (e.g., *Selenia* sp.; *Hemiaster* sp.)and foraminiferans (e.g., *Orbitolina*sp.; *Milioid* sp.;Adkins, 1928; Behrens, 1965; Clark and Morris, 2015). In some localities, LowerGRL beds grade laterally into

discontinuous rudist facies dominated by *Caprinid* sp. The presence or absence of rudist reef facies within vertical intervals of the Lower GRL was caused by changes in regional seawater chemistry, as well as localized changes in depth and water currents (Petta, 1977). The Lower GRL is topped by a regional "*Corbula* bed" (*Corbula* packstone–grainstone facies, this study), an ~15 cm marker unit dominated by the tiny bivalve *Eoursivivas harveyi* and commonly containing ripples (Scott et al., 2007; Ward and Ward, 2007). The Upper GRL is ~92–119 m thick in the study area and is dominated by m-scale marly–argillaceouswackstone to packstone beds and rare gypsum beds. The presence of evaporites is attributed to restricted circulation conditions shoreward of the Stuart City Reef (Fisher and Rodda, 1969). Rudist-dominated facies are present, but not common in the Upper GRL.

Individual beds within the GRL are heterogeneous and vary significantly laterally and vertically. Stratigraphic control has traditionally been maintained using the distinct fossil beds such as the *Corbula* and *Selenia* marker beds (e.g., George, 1952; Whitney, 1952; Ward and Ward, 2007; Clark and Morris, 2015). Central Texas Platform GRL strata are characterized by cyclic successions of facies grading from fine-grained mudstones and wackestones to fine- to medium-grained packstones and grainstones (Behrens, 1965; Clark 2003, 2005). Regional subsurface architecture forms clinoforms that span from the Llano Uplift to the Stuart City Reef (Cleaves, 1977; Braun, 2011).

All of the Trinity Group siliciclastic and carbonate units, including the GRL, were extensively faulted during the Miocene, creating the Balcones Fault Zone; a northeast–southwest trending zone of normal faults that extend from central to north Texas (Fig. 1; George, 1952; Horvorka et al., 1994). Miocene faulting occurred along preexisting zones of weakness in Paleozoic rocks along the Ouachita front (Collins, 1995). Most faults within the Balcones Fault

Zone are high angle and form a series of *en echelon* fault blocks in which relay ramps are common (Collins, 1995; Pantea et al., 2008).

2.2 Hydrostratigraphy

The Upper and Lower GRL have been subdivided into eleven hydrostratigraphic units (HSUs; Fig. 2)using theporosity-based classification system defined by Choquette and Pray (1970). Hydrostratigraphic units are stratigraphic divisions with distinct hydrologic characteristics (Maxey, 1964; Choquette and Pray, 1970). This definition was developed because there are various factors that affect aquifer fluid flow such as lithology, sedimentary structures, bioturbation, and structural features (Maxey, 1964; Choquette and Pray, 1970; Clark and Morris, 2015).The concept of HSUs was combined with the characterization of fabric and not-fabric selective porosity defined by Choquette and Pray (1970) for studies on the Edwards aquifer, which divided the Edwards aquifer into eight HSUs (I–VIII; Maclay and Small, 1976; Maclay, 1995; Barker and Ardis, 1996; Bumgarner et al., 2012). These studies on the Edwards aquifer severed as the basis for the subdivision of the GRL by Clark (2003, 2005) and Clark et al., (2009, 2014). The types of fabric-selective porosity within the GRL are in descending order of abundance: burrowed, bedding plane, moldic, shelter, and interparticle (Clark et al., 2009, 2014; Clark and Morris, 2015). The GRL also contains, in descending order of abundance, not-fabric selective fracture,vug,channel, cave, andbreccia porosity (Clark and Morris, 2015). All of the tidal-dominated strata of the GRL may contain one or more of these porosity types. Porosity created by biologic activity (i.e., burrowed) is the least studied feature within the GRL.

The Lower GRL was subdivided into six informal units by Blome and Clark (2014). The Lower GRL HSUs were named by Clark et al. (2014) as, in ascending order: the Honey Creek,

Rust, Doeppenschmidt, Twin Sisters, Little Blanco, and Bulverde HSUs (Fig. 2).The Upper GRL was informally subdivided into five HSUs by Clark (2003) and named by Clark et al. (2009). These five units are, in ascending order: the Lower Evaporate, Fossiliferous, Upper Evaporate, Camp Bullis, and Cavernous HSUs. Water well cores and petrophysical logs including gamma-ray, spontaneous potential, and resistivity logs were also used to identify the 11 HSUs in the subsurface (Blome and Clark, 2014; Pantea et al., 2014;Clark and Morris, 2015). Changes in welllog response are relative to changes in mud content and permeability; both of which are affected by the amount of bioturbation, as well as epikarst and fracture development (Zhou et al., 2002).

The Trinity aquifer is subdivided into the lower, middle, and upper Trinity aquifers. The upper Trinity aquifer is contained within the five Upper GRL HSUs (Ashworth,1983; Clark et al., 2009). The middle Trinity aquifer is contained within the six Lower GRL HSUs, the Hensell Sand, and the Cow Creek Limestone (Ashworth,1983; Blome and Clark, 2014; Pantea et al., 2014). The Hammett Shale is an impermeable aquitard between the middle and lower Trinity aquifers. The lower Trinity aquifer is contained within the Hosston and Sligo formations (Ashworth, 1983).

Due to the mud and siliciclastic material present in the GRL, wells within the Trinity aquifer commonly have a lower flow rate than wells within the Edwards aquifer (Maclay, 1995;Mace et al., 2000). However, the Trinity aquifer covers a much larger regional extent and rapid development within the Texas “Hill Country” between Austin and San Antonio has brought the aquifer to the attention of local groundwater users, water purveyors, and resource managers(Clark and Morris, 2015).

3.0 Methods

3.1 Field Methods

Fouroutcrop measured sectionswere made across the study area, covering all HSUsexcept the Little Blanco and Bulverde HSUs, which were examined in core (Supplemental Data Figs. 1–5).Outcrop sections were measured with a hand level and a Jacob's staff that was demarcated in decimal ft and extended up to 25 ft in length. Beds were described lithologically, sedimentologically, and ichnologically. Lithologies were described using the classification systemof Dunham (1962) for carbonates, the Embry and Klovin (1971) classification for rudist reef material, and the Wentworth (1922) classification scale for siliciclastics. Sedimentological features and ichnofossils were examined and described *in situ*; some representative ichnofossil samples were collected for photographs. Ichnofossils were described using morphology, surface textures, and burrow fill (e.g., Pemberton and Frey, 1982; Hasiotis and Mitchell, 1993). Additionally, two near-complete GRL coresfrom Camp Stanley, San Antonio, TX (MW9-CC, MW5-LGR), stored at the U.S. Geological Survey's Core Research Center in Denver, Colorado, were also described similarly to outcrop sections.

Ichnofabric indices were recorded in the field and used to interpret the percent amount of bioturbation as defined by Droser and Bottjer (1986). Ichnofabric index (ii) is a semiqualitative field interpretation of the amount of bioturbation within strata. This scale rates the amount of bioturbation from 1–6, where ii1 is a lack of bioturbation and ii6 is sediment that has been completely homogenized due to biologic activity.Ichnofabric indices of individual lithologic beds within HSUs were compared over the entire vertical extent of the GRL.

Additionally, field data collection was assisted by the use of an Apple iPad 2 loaded with geospatially registered 7.5-minute USGS topographic maps. Locations of visible and interpreted

contacts, faults and fractures, marker units, and other areas of interest were recorded using the integrated 3G assisted global positioning system (GPS) on the iPad, which is accurate to <1.5m if cellular data service is present, as over most of the study area. Major lithologic contacts were first identified and subadjacent strata were then described.

3.2 Laboratory Methods

One hundred petrographic thin section samples were taken from core MW9-CC in Bexar County, TX, the approximate location of which is indicated on Figure 1.Wagner Petrographic in Lindon, Utah produced the thin sections which were 24x46 mm in size and impregnated with clear epoxy. These thin sections were used to analyze mineralogy, cementation, micropaleontology, and microporosity.Analysis was conducted using an AmScope T490B-MT digital compound trinocular microscope with an integrated digital camera for pictomicrographs. Additionally, each thin section from MW9-CC was point counted using an Olympus BX53 microscope with an automated stepper stage controlled by PetrogLite 3.0 softwareto determine the matrix porosity of the sample and amount of cement (Conwy Valley Systems Ltd., 2011). Three hundred points were counted on each section and the results are summarized in Supplemental Data Table 1.

Plug samples from both outcrop and core were drilled and sent to Weatherford Internationalin Golden, Colorado for porosity and permeability testing via helium expansion. Core plugs were taken from GRL core MW5-LGR in Bexar County using a drill press with a diamond-tipped, 2.54 cm-diameter core bit (Supplemental Data Table 2). Outcrop plugs were taken in Kendall County using a cordless hand drill fitted with a 1.91 cm-diameter diamond core bit and water coolant tank (Supplemental Data Table 3). Helium expansion testing usedBoyle's

law to determine the porosity, permeability, and grain volume of a sample under 400 psi confining pressure (Winters et al., 1999). Results for porosity testing included ambient and neutron capture gamma-ray spectroscopy porosity, air and Klinkenberg permeability, and grain density.

4.0 Results

4.1 Lithofacies

In the study area, the GRL is subdivided into nine end-member lithofacies listed in deceasing order of relative abundance: (1) nodular and massive marly wackestone–packstone (Nwp); (2) cross-bedded argillaceouswackestone–packstone (Cwp); (3) fossiliferous grainstone (Fgs); (4) evaporitic mudstone (Ems); (5) *Corbula* packstone–grainstone (Cpg); (6) rudist-dominated floatstone (Rdf); (7) rudist-dominated bafflestone (Rdb); (8) laminated calcareous mudstone (Lcm); and (9) carbonate-cemented sandstone (Ccs).Lithofacies characteristics are summarized in Table 1 and illustrated in Figures 3 and 4. The described lithofacies are specific to the study area and do not include the full extent of previously published depositional environments for the GRL (e.g.,Lozo and Stricklin, 1956; Behrens, 1965; Perkins, 1974; Pittman, 1989; Mancini and Scott, 2006).

4.2 Ichnology

Ichnofossils are common in the GRL and are pervasive within most beds on the Central Texas Platform.Marine organisms react to a variety of physicochemical factors such as substrate composition,nutrient availability, salinity, turbidity, temperature,and oxygen (e.g., Ekdale and Bromley, 1984a,b; Bromley and Ekdale, 1986; Uchman, 1995). Ichnofossils are listed in

decreasingrelative order of abundance and include: (1) *Thalassinoides*;(2) *Palaeophycus*;(3) *Planolites*, (4) *Ophiomorpha*, (5) rhizoliths,(6) *Serpulid* traces, and (7) *Cruziana*. The relationships between ichnofossils and lithofacies are summarized in Table 1.

4.2.1Thalassinoidesisp.(Fig. 5A–C)

Thalassinoides are unlined, three-dimensional boxworks of cylindrical burrows.These traces range from ~0.5–2.5 cm in diameter within the GRL. Some burrows are >4 cm in diameter due to solution enhancement in locations proximal to karstic features. Infill of burrows is similar to surrounding matrix or overlying beds and may consist of mudstone or wackestone–grainstone.*Thalassinoides*in the GRL are commonly multigenerationally tiered, with burrow density decreasing upsection in individual beds (Bromley and Ekdale, 1986).These networks comprise the majority of ichnofossils in all GRL lithofacies, but are most prevalent in wackestone–packstone facies.Cunningham and Sukop (2012) showed that abundant *Thalassinoides* ichnofabrics in the Edwards Group affected lateral fluid flow within beds, but the mudstone and siliciclastic sediment within the GRL complicates such direct interpretations. Computer modeling has also shown that *Thalassinoides* networks begin to continuously interconnect when burrows comprise as little as ~10% of the strata (La Croix et al., 2012). These *Thalassinoides* networks provide the majority of bioturbation-influenced fluid pathways within the GRL.

4.2.2 Palaeophycusisp. (Fig. 5D)

Palaeophycus are mud-lined, cylindrical burrowswith infill similar to the matrix or overlying unit. These traces range from 0.5–2.0 cm in diameter within the GRL. The mud lining

is thin (~1 mm), micritic, and commonly dark yellow (Fig. 5D). *Palaeophycus*are commonly found associated with,and have similar sediment infill to,*Thalassinoides* networks. The infill within the traces shows no evidence of active backfilling such as meniscae and was likely deposited with overlying sediment. *Palaeophycus* is most often found overlaying significant *Thalassinoides* networksin beds with less bioturbation.Because of their similar morphology to and proximal associationwith *Thalassinoides*,these *Palaeophycus* were likely made by the same tracemakers. *Palaeophycus*are commonly found above *Thalassinoides* networks in marly wacketone-packstone facies. *Palaeophycus*commonly havecoarse-grained, permeable infill and likely act as fluid pathways.

4.2.3 Planolitesisp. (Fig. 5E–F)

Planolities are unlined, mud-filled,cylindricalburrows oriented parallel to bedding planes (Fig. 5E). These burrows vary in diameter slightly along their length and range from 0.2–1.5 cm in diameter.*Planolites*are commonly found isolated from *Thalassinoides* networks within beds with relatively low bioturbation. The matrix of these beds varies from mudstone to packstone and is commonly argillaceous, though *Planolites* isfound associated with detrital conglomeratic material in one bed (Fig. 5F). *Planolites*have smooth walls and rarely branch or overlap.The infill of *Planolites* is muddy and distinct in color and fabric from the surrounding matrix and overlying units. The muddy infill of *Planolites* within the GRL means that they will act as fluid barriers.They are common in beds near the top of the Lower GRL and likelydo not play a significant role in overall fluid flow.

4.2.4 Ophiomorphaisp. (Fig. 6A–B)

Ophiomorpha are pellet-lined,cylindricalburrows that may branch and range from 2.5–3.0 cmin diameter (Fig. 6A).Burrow infill is similar to surrounding matrix and pellets are composed of mud, but may contain various small clasts. *Ophiomorpha* are commonly horizontally-oriented, found associated with *Thalassinoides* networks, and may grade into unlined burrows within units. Similar to *Thalassinoides*, *Ophiomorpha* may branch and be multigenerationally tiered(Fig. 6B; Bromley and Ekdale, 1986). These ichnofossilsare found within higher-energy crossbedded wackestone-packstone facies in the Upper GRL and within units with larger clast sizes on average.These traces were likely made by the same tracemaker as *Thalassinoides* and *Palaeophycus*. The mud pellets are simple peloids and are created by the tracemaker to increase the structural integrity of the burrow (Uchman, 1995;Vaziri and Fürsich, 2000). Many *Thalassinoides* burrows within the GRL may have originally been *Ophiomorpha*, but have been altered by subsurface and meteoric water flow, removing evidence of the pelleted lining (Bromley and Frey, 1974; Myrow, 1995). Also similar to *Thalassinoides*, these traces likely act as significant fluid pathways in both the Upper and Lower GRL, particularly within crossbedded strata. Additionally, *Ophiomorpha*-dominated ichnofabrics have been shown to be the primary hydrologic driver of the similar karstic Biscayne aquifer of southern Florida (Cunningham et al., 2009)

4.2.5 Rhizoliths (Fig. 6E–F)

Root traces have several different forms within the GRL, and include rhizoliths, rhizohaloes, and rhizocretions. Generally, these are tapered traces that extend downward from subaerial exposure surfaces into underlying strata and may crosscut underlying bedding surfaces. True rhizoliths are found in muddy units and have distinct downward tapering morphologies and

wood-like textures in cross-section (Fig. 6E). Some rhizoliths have a light-colored rim around the entire structure called rhizohaloes (Fig. 6E). Some beds show light colored discoloration interpreted to be rhizohaloes with no remaining fossilized woody material. Rhizocretions have a nodular texture that appears as interlocking and overlapping spheres that contain root hair traces in cross section (Fig. 6F). Nodular beds showing rhizocretions are typically <0.5m thick. Rhizoliths are associated with only insipient soil development in the study area, but enough development to concentrate clay minerals via illuviation in subaerially exposed horizons (Kraus and Hasiotis, 2006; Smith et al., 2008; Hasiotis and Platt, 2012).Beds and surfaces suggesting subaerial exposure and showing rhizoliths are rare in the study area, but previous studies have shown that such beds increase in abundance northward on the Central Texas Platform (Lozo and Stricklin, 1956; Perkins, 1974; Ward and Ward, 2007). Rhizoliths are therefore potential hydrologic indicators as the increased amount of clay may act as a barrier to fluid flow.

4.2.6Serpulid tubes (Fig. 6C–D)

Serpulid tubes are carbonate cement-lined, cylindrical, coiled tubes filled with mudstone that are oriented parallel to bedding planes. Single tubes may be tens of cm long and may coil on themselves several times (Fig. 6C). The tubes have a distinct brown-tan color with transverse striations and mud infill that is concentrically laminated (Fig. 6D). Serpulid tubes are commonly found attached to bivalve and gastropod shells. The tubes may have been filled with sediment after burial and the presence of sparry infill acts as a geopetal in thin section (Fig. 6D). Similarmodern tubes are created by annelid worms of the genus *Serpula*(Vinn et al., 2008).These tubes are found within muddy, fossiliferous units that consist primarily of nodular marly wackestone and packstone and play a very minor role in fluid flow.

4.2.7Cruziana isp. (Fig. 6G)

Cruziana are bilobate furrows with a medial ridgeand transverse, ridged striations that gently curve back away from the direction of travel. *Cruziana* traces in the GRL average ~13 cm wide and range from 47.4–59.3 cm long (Fig. 6G). These furrows are ~2–3 cm deep with preserved mounding and drag marks along the sides of trace. All observed *Cruziana* are associated with crossbedded wackestone–packstone at a single location in Comal County and several of the traces overlap on a single bedding surface. Other ichnofossils, such as *Thalassinoides,* are relatively rare in the associated strata. The tracemaker for these *Cruziana* in the GRL has previously been interpreted as horseshoe crabs (Ward and Ward, 2007). This study; however, interprets the tracemaker as a different large arthropod or possible isopod because horseshoe crab trackways generally lack distinct scratch marks such as the curved striations seen in these trackways, but commonly have individual limb traces (Babcock et al., 2000). Although these traces are associated with otherwise transmissive facies, the location of these trackways along bedding planes and their limited preserved extent indicates that these ichnofossils have no effect on fluid flow.

4.3 Ichnofabric index analysis

The GRL is muddy and has low intergranular porosity; therefore, fluid pathways are often larger-scale features such as faults and fractures, ichnofossils, and molds. Ichnofabric indices (ii), as a measure of ichnofossil density and overall bioturbation, can be used as hydrologicindicators within the GRL and similar karstic aquifers (Fig. 7).An ii1 unit will have no bioturbation (Droser and Bottjer, 1986) and fluid flow will be restricted to intergranular porosity

if faults and karstic development are not present. Beds with ii2 have less than 10% of their total volume bioturbated; such beds within the GRL commonly contain *Palaeophycus*,*Planolites*, andvisible sedimentary structures (Fig. 7A). Beds with ii3 have 10–40% percent of their total volume bioturbated; most GRL ii3 beds are dominated by *Thalassinoides* networks and have few to no visible sedimentary structures (Fig. 7A). Beds in the GRL that are ii4 have 40–60% of their total volume bioturbated, are dominated by *Thalassinoides* networks, and generally have no sedimentary structures visible (Fig. 7B). Beds with ii5 have over 60% of their volume bioturbated; some individual *Thalassinoides* are visible within these beds (Fig. 7C). Beds that are completely homogenized and nodular in appearance are assigned to ii6 and dominated by cryptobioturbation (Fig. 7D).

Thalassinoides-dominatedichnofabrics become interconnected throughout beds at ii3 and above (La Croix et al., 2012). Beds within the wackstone-packstone facies in the GRL that have ii3–4 contain*Thalassinoides* networks that may act as fluid pathways. In fine-grained facies; however, *Thalassinoides* are often infilled with mud and do not increase overall porosity. Beds that are ii5–6 are generally homogenized and donot transmit fluids easily. Ichnofabric index must therefore be examined in conjunction with lithology, porosity, and permeability characteristics of stratato infer whether beds are transmissive or confining. The ii trends, porosity characteristics, and interpreted transmissivity within the individual HSUsof the Lower and Upper GRL are described below (Fig. 8) and summarized in Table 1.

4.3.1 Lower Glen Rose Limestone

The Lower GRL is primarilycharacterized by coarsening-upward successions of marly wackestone to packstone facies that grade laterally into discontinuous rudist-dominated

bafflestone and floatstone facies (Fig. 8). The Lower GRL has been subdivided into six HSUs, which have been designated as either transmissive or confining based on porosity characteristics, as well as lithology (Table 1; Clark et al., 2014; Clark and Morris, 2015). Generally, transmissive units have been defined based on the presence of wide-spread fracture porosity and karstic development; however, trends in bioturbation-influenced porosity can also be seen in these units (Clark et al., 2014) The Lower GRL includes, from stratigraphically lowest to highest, the Honey Creek, Rust, Doeppenschmidt, Twin Sisters, Little Blanco, and Bulverde HSUs.

Transmissive HSUs—Lower GRL transmissive units include the Honey Creek, Doeppenschmidt, and Little Blanco HSUs. These HSUs consist of tidal-dominated, m-scale successions of coarsening-upward nodular and massive marly wackestone–packstone beds with ii4–5 and some identifiable *Thalassinoides* networks (Table 2; Fig. 9). These successions grade upsection into marly wackestone–packstone with ii3–4 characterized by open and wackestone–packstone-filled *Thalassinoides* networks. Some beds of laminated calcareous mudstone with ii1 are located at the base of successions and grade upsection into the more typical nodular wackestone with ii4–5 (Table 2; Fig. 9).In some locations, transmissive HSUs grade laterally into discontinuous patch reefs consisting of rudist-dominated floatstone and bafflestone having ii1–ii2, with some *Planolites* observed in the mudstone matrix of floatstones. Although the tidal-dominated strata of transmissiveHSUs have less permeability than the rudist facies, bioturbation-influenced porosityis likely connected throughout the units and is a major component of this unit's transmissivity.

While transmissive strata share the above characteristics, unique features are observed in each HSU. The bottom ~6.7 m of the Honey Creek HSU (Fig. 9) consists of the typical successions described; however,the top ~3 m of the unit has lower ii and consists of interbedded

laminated calcareous mudstone and nodular wackestone with ii1–2 and containing *Palaeophycus*with some *Thalassinoides* networks. While defined as a transmissive unit, most of the bioturbation-influenced porosity of the Honey Creek HSU appears to be restricted to the bottom 6.7 m of the unit in beds with ii3–4. Most fracture and karstic development also appears in the lower portions of the Honey Creek HSU (Clark and Morris, 2015). The Doeppenschmidt HSU also consists of wackestone–packstone facies typical of transmissive units, but contains less mud than the Honey Creek HSU and should have higher permeability as a result(Fig. 8). The Little Blanco HSU contains some successions that grade upward into crossbedded wackestone–packstone with ii1–2. Therefore, fluid flow is restricted to intergranular porosity and is lowin these less-bioturbed units. Additionally, fluid flow is also likely restricted in the top ~1.8 m of the Little Blanco HSU where muddier wackestone units are interbedded with ii1–2 laminated calcareous mudstone.

Confining HSUs—Lower GRL confining units consist of the Rust, Twin Sisters, and Bulverde HSUs (Fig. 8). Confining HSUs usually consist of m-scale beds of nodular, marly wackestone with ii5–6 that are thoroughly homogenized by pervasive cryptobioturbation with some identifiable *Thalassinoides*(Table 2; Fig. 10). Unlike transmissive HSUs, confining units generally do not display coarsening upward trends, contain more mud, and show less fracture porosity. Similar to transmissive units, confining HSUs in some locations grade laterally into discontinuous patch reefs consisting of rudist-dominated floatstone and bafflestone having ii1–ii2 (Fig. 8). These patch-reefs have high moldic and fracture porosity, but because of their lateral isolation within otherwise confining strata they cannot transmit water within the HSU. These patch reefs may; however, transmit water vertically between transmissive units(Hunt and Smith, 2010).

While the Twin Sister HSU is typical of these confining units (Fig. 10), the Rust HSU displays some coarsening upward successionssimilar to transmissive units. Burrow infill in the Rust HSU ranges from wackestone–packstone, and the uppermost beds contain *Palaeophycus*and mud-filled *Planolites*. These mud-filled ichnofossils in the Rust HSU do not increase bioturbation-influenced porosity as much as seen in transmissive units. The Bulverde HSU is complex—it consists mainly of coarsening-upward successions of nodular and crossbedded wackestone–packstone withoverall well-developedbioturbation-influenced porosity (ii4-5) similar to transmissive units. However, it contains interbedded laminated calcareous mudstoneintervals (ii1) at the base and is capped by *Corbula* packstone–grainstone (ii1), both of which severely restrict fluid flow. Although the Bulverde HSU has been classified as a confining unit, thetransmissive middle portion contains well-developed biogenic and moldic porosity and may transmit significant amounts of water.Thus, the Bulverde HSU may be better classified as a semi-confining unit.

4.3.2 UpperGlen Rose Limestone

The Upper GRL primarily consists of coarsening upward successions of marly wackestone to packstone facies similar to the Lower GRL, but contains abundant evaporites andfew rudist dominated patch reefs (Table 2; Fig. 8). Conditions during the deposition of the Upper GRL appear to have never fully returned to the normal marine conditions seen in the Lower GRL after the deposition of the *Corbula* bed (Fisher and Rodda, 1969). The Upper GRL has been subdivided into five HSUs: the Lower Evaporite, Fossiliferous, Upper Evaporite, Camp Bullis, and Cavernous HSUs (Clark, 2005; Clark et al., 2009). Transmissive HSUs are associated with significant evaporitic beds and karstic development. Confining units in the Upper GRL are

lithologically and ichnologically similar to transmissive units in the Lower and are interbedded with the karstic transmissive units.

Transmissive HSUs—Upper GRL transmissive units includethe Lower Evaporite, Upper Evaporite, and Cavernous HSUs. TheseLower Evaporite and Upper EvaporiteHSUs areeach ~3 m thick and characterized by evaporitic mudstone with ii1–2 andpervasive dissolution features in both evaporites and carbonates (Table 2).Both the Lower and Upper Evaporite HSUs also contain significant moldic porosity and karstic development from the dissolution of evaporitic minerals (Clark, 2005; Clark et al., 2009). These Evaporite HSUs were deposited in brackish conditions preventing wide-spread bioturbation in this unit (Fisher and Rodda, 1969).

The Cavernous HSU overlies the Camp Bullis HSU and is highly transmissive because of significant karstic and cave features present in the subsurface (Clark, 2005). Defined in core and through geophysical analysis (Clark, 2005) in northern Bexar County, TX (see Fig. 1), the Cavernous HSU is typically less than 10.5 m thick, has a limited lateral extend and is not present at the surface through most of the study area. This HSU consists of marly wackestone–packstone successions similar to transmissive units in the Lower GRL, but has been significantly faulted and fractured. The high permeability of the overlying Edwards Group has introduced meteoric water into these faults and fractures creating karstic features (Smith et al., 2005; Clark, 2004). Pervasive solution enhancement has destroyed most evidence of bioturbation in this unit, particularly in close proximity to faults and fractures. Within the GRL, the Upper GRL HSUs display more solution enhancement due to the high infiltration rates of the overlying Edwards aquifer (Maclay, 1995; Smith et al., 2003; Clark, 2004). The steep, near vertical orientation of the Balcones Fault Zone faults has allowed for the introduction of meteoric water deep within the

aquifer, which has infiltrated laterally from the faults following interconnected *Thalassinoides* networks and other ichnofossils and molds within the GRL.

Confining HSUs—The Upper GRL confining units are the Fossiliferous and Camp Bullis HSUs (Fig. 8). Similar to Lower GRL transmissive units, the Fossiliferous and Camp Bullis HSUs consist of coarsening-upward successions that grade from nodular, marly wackestone with ii5–6 dominated by pervasive cryptobioturbation to marly wackestone–packstone with ii3–4 and pervasive *Thalassinoides* networks (Table 2; Fig. 11). These *Thalassinoides*are commonly infilled with wackestone–packstone from overlying units. Additionally, sequence bases may contain thin beds of laminated calcareous mudstone with ii1. These HSUs share many similarities with the transmissive units of the Lower GRL and contain well-developed burrow and bedding-plane porosity with some fracture development (Fig. 11; Clark, 2005; Clark et al., 2009). These units,however, are significantly less permeable than the evaporitic and Cavernous HSUsbecause of their mud content and lack of dissolution features and fractures (Clark, 2005; Clark et al., 2009).

The Fossiliferous HSU is fairly muddy but coarsening-upward patterns of successions are observed, unlike most confining units in the Lower GRL. This HSU contains significant moldic porosity due to the dissolution of shell material, as well as well-developed bioturbation-influenced porosity. This unit, however, does not transmit water as readily as the overlying and underlying evaporite units. Numerous seeps and springs are found at the top of this unit, indicating diverted flow of meteoric, similar to confining units in the Lower GRL. The Fossiliferous HSU does grade laterally into rudist patch reef strata with high fracture and moldic porosity in northern Bexar County.

The Camp BullisHSU (Fig. 11)contains less mud than the other HSUs and successions within it grade from typical cryptobioturbated beds seen in the Fossiliferous HSU to marly wackstone–grainstone with ii3–4 with abundant *Thalassinoides* and *Ophiomorpha*. The grainstone at the top of many of these successions shows some crossbedding and has ii1 and is well-cemented leading to low intergranular porosity. Similar to transmissive units in the Lower GRL, the muddier ii5–6 beds at the base of successions in the Camp Bullis HSU likely prevent significant vertical fluid flow but water is transmitted laterally in overlying beds with ii3–4 to seeps and springs and to fractured areas.

The Fossiliferous and Camp Bullis HSUs have previously been defined as confining units because of diversion of ground and meteoric water seen at the surface of these units (Clark, 2005; Clark et al., 2009). This is likely because of the comparatively high permeability seen in the evoporitic and Cavernous HSUs, as well as the large amount of meteoric water that can quickly infiltrate the overlying Edwards Group. However, the similarity of these two units both ichnologically and lithologically to Lower GRL transmissive units and well developed porosity likely allows for the transmission of significant amounts of water. These two units may; therefore, be better described as “semi-confining HSUs”.

4.4 Solution enhancement of ichnofossils

Solution enhancementin the GRL has increased connectivity of fractures and burrows and caused autoclastic brecciation and cavern development in many cases. Multiple stages of solution enhanced features are preserved and forming in the GRL (Fig. 12). In the typical coarsening upward sequence, most ichnofossils are filledwith sediment sourced from overlying strata that is coarser than the surrounding matrix.This initial condition is shown in figure 12 (T_1).

This focuses water flow, particular from meteoric water, through the ichnofossil networks and will dissolve the matrix surrounding the burrow over time (Fig. 12; T_2). Meteoric water is not in equilibrium with the carbonate content of the surrounding matrix and will thus widen and further interconnect the burrow networks across the three-dimensional extent of the bed (Fig 12; T_3). These solution-enhanced burrow networks may subsequently either be filled with sediment (Fig 12; T_{4a}) or continue to have the matrix dissolved by infiltrating meteoric and ground water (Fig. 11; T_{4b}). If exposed, infilled solution enhanced burrows may weather differentially from the surrounding matrix and be preserved in positive relief (Fig. 12; T_{5a}). Alternatively, dissolution may continue until the matrix cannot support the overburden and the sediment compacts, evidenced by a bed of brecciated sediment (Fig. 11; T_{5b}).

Solution enhancement features are most significant in the GRL within close proximity to faults and fractures and in beds associated with karstic development. The Upper GRL HSUs are more solution enhancedthan Lower GRL HSUs due to the high infiltration rates of the overlying Edwards aquifer (Hanson and Small, 1995; Maclay, 1995; Clark, 2004). The near vertical faults of the Balcones Fault Zone transmitted meteoric water into the subsurface where it infiltrated laterally into the strata along interconnected *Thalassinoides* networks and other ichnofossils and molds.

5.0 Discussion

Ichnologic assessment is important in aquifer and reservoir characterization,however, most studies have been conducted in siliciclastic units (e.g., Keswani and Pemberton, 2007; Tonkin et al., 2010; Gingras et al., 2012). Bioturbation commonly decreases porosity and permeability in both siliciclastic and carbonate aquifers that contain significant intergranular

flow (e.g., Gingras et al., 2004; 2012).Karstic aquifers such as the Edwards and Trinity Groups; however, cannot transmit significant quantities of fluid through interparticle porosityand rely on bioturbation to create porosity and lateral fluid pathways (e.g., Mathews, 1967; Gingras et al., 1999; Cunningham and Sukop, 2011; Baniak et al. 2013; Golab et al., 2015).Although previous authors have conducted ichnological assessment of some carbonate hydrocarbon reservoirs (e.g., Gingras et al., 1999, 2004; La Croix et al., 2011; Baniak et al., 2013), thebiogenic aspect of karstic aquifers has been overlooked in the literature (Cunningham et al., 2009; Cunningham and Sukop, 2011, 2012; Golab et al., 2015; Clark et al., 2016). The GRL is a dual-permeability system and absent fracture and karstic porosity, ichnofossils with coarse-grained infill are the primary fluid pathways throughout most strata and are a significant factor in directing water between major faults and karstic features. All GRL beds have been shown to produce hydraulic head in water wells, even those that have been classified as confining and lack significant karstic features (Clark, 2003; Hunt and Smith, 2010).

5.1 Glen Rose Limestone depositional environment

The development of *Thalassinoides* networks is particularly common and abundant in tidal-dominated carbonate platform strata (e.g., Myrow, 1995). Common *Thalassinoides* tracemakers in modern carbonate settings include *Callianassa* sp., decapod crustaceans and other arthropods (Sheehan and Schiefelbein, 1984; Myrow, 1995). Similar to *Thalassinoides*, *Ophiomorpha* is common in high-energy, shallow marine systems (Uchman, 1995). *Ophiomorpha* are often found associated with rapid deposition in a high-energy, wave-dominated environment.

The Lower GRL was deposited in shallow subtidal–supratidal environments with some terrestrial input. Diversity of the fossil assemblage indicates normal ocean salinity (Behrens, 1965). The presence of dasycladaceae algae in thin section indicates < 30 m of water depth during deposition (Riding, 2007). Root traces and terrestrial plant material found in some beds indicate that sea-level fluctuated enough to subaerially expose the sediment at times during deposition. Siliciclastic material was sourced from the Llano Uplift by fluvial systems (Behrens, 1965), though freshwater input does not appear to have been significant enough to create widespread brackish conditions and decrease faunal diversity (Cleaves, 1977). The Lower GRL is capped by the regional *Corbula* bed in which the lack of fossil diversity has been previously interpreted to indicate highly restricted conditions behind the Stuart City Reef, leading to hypersaline conditions (Behrens, 1965). This restriction was likely caused by a significant drop in sea level, completely isolating the Central Texas Platform from oceanic water input leading to brackish conditions (Behrens, 1965).

The Upper GRL is characterized by higher depositional energy facies and evaporites. Restricted conditions on the landward side of the Stuart City Reef likely became widespread during the deposition of the *Corbula* packstone-grainstone facies (Fisher and Rodda, 1969). The laterally extensive evaporite units in the Upper GRL correlate to unconformities on reef deposits to the south and southeast (Bebout et al., 1977; Schlager, 1989). Regional evaporitic conditions created the Lower and Upper Evaporite HSUs of the Upper GRL.

Rudist-dominated facies were deposited as isolated patch reefs. These rudist-dominated patch reefs are common in the Lower GRL and rare in the Upper GRL. These reefs have a limited lateral extent of less than 300 m across (Petta, 1977). The talus slopes of rudist patch reefs commonly form on top of packstones and grainstones that are deposited laterally from the

associated reef. Previous studies on rudist reefs in the GRL showed that *Caprinid* sp. likely formed in <5 m water depth (Perkins, 1974; Petta, 1977).

5.2 Hydrologic effects of Thalassinoides-dominated ichnofabric

Strata within the GRL contain significant amounts of mud and cement, leading to low intergranular porosity. Faults and karstic features have created most of the vertical fluid pathways within the Trinity aquifer and allow meteoric water to enter the subsurface (e.g., George, 1952; Maclay and Small, 1976; Horvorka et al, 1994; Faith, 2004;Pantea et al., 2008). Lateral fluid flow within beds; however, is more difficult to characterize and is primarily controlled by *Thalassinoides* networks. Baniak et al. (2013) showed that *Thalassinoides*-dominated ichnofabrics are more commonly interconnected horizontally and only become vertically connected throughout a stratum after pervasive bioturbation. Such *Thalassinoides*-dominated ichnofabricsact as conduits for fluids in the absence of faults or karstic development. These ichnofossils were also the precursor to most vug and channel porosity due to solution-enhancement of burrow networks, and facilitated the development of widespread moldic porosity.

La Croix et al. (2012) showed that *Thalassinoides* networks begin to become interconnected throughout the three-dimensional extent of a stratum at ii3 and above. This model matches well with the ichnofabric index trends seen in this study, where ii3–4 beds in the GRL are interpreted to be the most transmissive units.In *Thalassinoides*-dominated ichnofabricslateral connectivity may exist at ii3, though vertical connectivity is generally only associated with ii5 and above(Baniak et al., 2013). Cunningham and Sukop (2010) showed that the *Thalassinoides*-dominated ichnofabrics of the overlying Edwards aquifer significantly increase permeability;

however, the amount of mud and heterogeneity observed in the GRL makes this correlation less direct. Defining fluid pathways within theGRL requires the combined use of ichnofabric indices, lithology, and structural features. Each of the eleven GRL HSUs is unique, but most transmissive units show similar trends within beds of upward coarsening in grainsize and decreasing ichnofabric indices (Fig. 9–10).

While each HSU displays some distinct hydrologic characteristics, most contain successions of decreasing-upward ii and show that biogenic fluid flow is restricted on a smaller scale within each GRL fifth-order sequence (Table 2; Figs. 9 and 11). The bases of successionsarecommonly muddy andconsist of nodular strata with ii5–6. The ichnofossils at the bases of successions are dominated by multigenerationally tiered *Thalassinoides* networks. Much of the nodular appearance of these basal beds is attributed to cyrptobioturbation. The middle portionsof successionsare commonly characterized by strata with ii3–4 composed of *Thalassinoides* networks as well as *Ophiomorpha,* and occasional *Palaeophycus*and *Planolites.*These zones with ii3–4 are the most prominent area of biogenic fluid flow within the GRL as they are both interconnected throughout the strata and are commonly filled with infill coarser-grained than the surrounding matrix (La Croix et al., 2012; Baniak et al., 2013). The tops of successionsmay consist of massive to crossbedded packstone–grainstone with ii1–2 and contain *Palaeophycus*and *Planolites* as dominant traces. Fluid flow within these upper, low ii strata is restricted to intergranular pore space.While these upper beds contain less mud, they have significant amounts of sparry cement; therefore, permeability is still low.

5.3 Quantifying the hydrologic characteristics of dual-permeability systems

Quantifying changes in aquifer permeability and porosity is difficult as most available laboratory methods, such as point-counting and helium-expansion porosity testing, were developed to measure intergranular pore space of the matrixmaterial and do not accurately characterize the large-scale fluid pathways seen in the GRL (Fig. 8 and Table 1). No direct correlation could be observed between point-counted matrix porosity and the larger-scale hydrologic trends observed within the HSUs (Supplemental Table 1). Average porosity from point counts averaged only 5.27%, and showed no significant difference between different facies. Helium-expansion porosity and permeability are also limited to small-scale matrix and fracture porosity, but some observable trends could be seen between lithofacies (Supplemental Tables 2–3). The results from the helium expansion testing averaged 17.6% porosity and 14.6 mD permeability. Crossbedded wackestone–packstone (0.69 mD) and evaporitic units (0.049) have the lowest measured permeability whereas fossiliferous grainstone (39.4 mD) has the highest.

The hydrologic flow observed in the GRL (Hunt and Smith, 2010) is at least 3 orders of magnitude greater than can be explained by permeability values measured from helium expansion and point counting of the matrix. The most extreme example of this is within the Lower and Upper Evaporite HSUs, which are interpreted to have the highest permeability in the GRL based on fluid flow, but contain the lowest measured helium expansion permeability values. This discrepancy in the Evaporite HSUs is likely due to abundant fractures. The other HSUs within the GRL; however, are dominated by ichnofossils instead of fractures. Unlike fracture-dominated dual-porosity systems, bioturbation-influenced pore systems are more heterogeneous and create variable flow depending on the difference in permeability between the matrix and burrow fill (Gingras et al., 1999; Baniak et al., 2013).

Studies by Cunningham et al. (2009) and Cunningham and Sukop (2011) on the karstic Biscayne aquifer of southern Florida used x-ray tomography scans of full-diameter core samples (~10 cm diameter) to measure the porosity of large-scale burrow networks. These studies then used lattice Boltzmann equations to estimate vertical and lateral permeability (Cunningham et al., 2009). Although such datasets are, as of yet, unavailable for this study, the lithological and ichnological similarity of the GRL with the Biscayne aquifer means that values for the large-scale burrow permeability can be approximated for GRL strata.Cunningham et al. (2009) and Cunningham and Sukop (2011) estimated permeability values greater than five orders of magnitude higher than any previous study on the Biscayne aquifer system. Strata with ii3 were shown to have an average permeability of 8.2 x 10^7mD, ii4 units averaged 2.7 x 10^9 mD, and ii5 strata averaged 8.6 x 10^9mD (Cunningham et al., 2009).Although these numbers cannot be directly related to the GRL because the Biscayne aquifer's *Ophiomorpha*-dominated strata contain less mud and siliciclastic material, they illustrate the effect large-scale bioturbation-influenced porosity can have on karstic aquifer systems and may be used as a template for future studies on the Edwards (Cunningham and Sukop, 2012) and Trinity aquifers. Furthermore, the Biscayne may be more lithologically and ichnologically similar to the Edwards Group, as both contain less mud and siliciclastic content than the GRL.

5.4 Solution-enhancement and karstic development

The solution enhancement of ichnofossils has also played a role in the development of GRL fluid flow. Introduction of meteoric water likely began with the exhumation of strata along the normally faulted Balcones Fault zone during the Miocene (Horvorka et al. 1994; Clark et al. 2009).Solution enhancement by dissolution of material in contact with fluid pathways is a

prominent feature in carbonate systems (e.g., Mylroie and Carew, 1990), and many GRL fluid pathways show evidence of having been enhanced by meteoric and groundwater flow.Dissolution in pre-existing three-dimensional geometric patterns of ichnofossils has significantly increased the lateral and vertical permeability of most transmissive HSUs by further interconnecting *Thalassinoides* networks and widening fluid pathways. Within areas where such dissolution is extensive, complete dissolution of ichnofossils results in the formation of karstic features.

Karstic development, while primarily controlled by faulting and fracturing (Horvorka et al, 1994; Maclay, 1995; Faith, 2004), is influenced also by the presence or absence of ichnofossils (Keswani and Pemberton, 2007). Hydrostratigraphic units within the GRL that contain significant fault and fracture porosity have commonly been defined as the most transmissive(Clark, 2003, 2005; Clark et al., 2009; Clark et al., 2015). Additionally, karstic features associated with fractures are significant fluid pathways and catchments(Clark, 2003, 2005; Faith, 2004; Pantea et al, 2014). Bedswith well-developed biogenic networks transmitted water laterally away from faults and fractures. This action aided in karstic development within transmissive bioturbated beds.These features can be observed easiest in the Lower GRL Honey Creek HSU and was a likely major component in the development of the Upper GRL Cavernous HSU.

6.0 Conclusions

Large-scale bioturbation-influenced porositysuch as burrows, borings, and nodular preservation of bioturbationis one of several factors that affect fluid flow within the GRL of the Trinity aquifer; however, its significance in karstic aquifers and reservoirs has not been

exploredby many authors. While faulting and fracturing and karstic development are commonly the most prevalent fluid pathways within aquifers that lack significant intergranular porosity and permeability, biogenic fluid pathways (i.e., burrows) act as conduits to move fluids laterally between faulting and fracture features. Bioturbation-influenced porosity is of particular interest to carbonate aquifers, many of which contain interconnected *Thalassinoides* or *Ophiomorpha* networks (e.g., Mazzullo and Chilingarian, 1996;Cunningham et al., 2009).

Previous studies have shown *Thalassinoides*-dominated ichnofabrics tend to increase the lateral connectivity of beds by creating interconnected 3-dimensional fluid pathways of either open burrows or burrows with permeable fill (e.g.,Cunningham and Sukop, 2012; Baniak et al., 2013). The muddy and siliciclastic input present during GRL deposition; however, complicates such a straight-forward correlation. Transmissivebeds in the GRLbeds have ii3–4 and burrows are commonly open or have permeable fill. Beds with ii5–6 are commonly muddy and heavily homogenized, and restrict fluid flow. Additionally, grainstone beds commonly have ii1–2 and are cemented, restricting fluid flow to low intergranular flow.

Characterizing the lateral fluid pathways requires the integration of lithology, structural and karstic features, and ichnology. The overall transmissive or confining nature of hydrostratigraphic units in the GRL depends on the ichnofabric index, fracture density, and karstic features both within the beds and in the overall stratigraphy. For example, confining beds in the Upper GRL are lithologically and ichnologically similar to transmissive beds in the Lower GRL (see figs. 9 and 11). The Upper GRL contains evaporites and significantly more karstic development than the Lower GRL, meaning that transmissive units are more commonly characterized by evaporites with significant dissolution features. Although the confining units in the Upper GRL contain significant bioturbation-influenced porosity and less mud than Lower

GRL transmissive units, they are significantly less permeable than the evaporitic and Cavernous HSUs and divert water to seeps and springs. All of these Upper GRL units; however, likely transmit water laterally and the two Upper GRL confining units may; therefore, be better described as “semi-confining HSUs”.

Analysis of fluid pathways is further complicated by the solution enhancement of ichnofossils by meteoric water. Solution enhancement features are most significant in close proximity to faults and fractures and within the GRL, the Upper GRL displays more solution enhancement due to the high infiltration rates of the overlying Edwards aquifer (Maclay, 1995; Smith et al., 2003; Clark, 2004). Solution enhancement greatly increases lateral and vertical connectivity and permeability of units and, in some beds, was the first step toward development of larger-scale karstic features.

Ichnofabric assessment of karstic aquifers may also be of benefit to hydrocarbon exploration. Large-scale vug porosity is a common feature in karstic reservoirs and aquifers and may have been mediated by biologic activity (Mazzullo and Chilingarian, 1996;Gingras et al., 1999; Cunningham et al., 2009; Baniak et al., 2013). Understanding the interaction of burrows and molds that may lead to such porosity may become increasingly important as part of reservoir characterization. The shelf carbonates of south TX have been explored for oil and gas plays with active fields targeting the Edwards Group and Austin Chalk Formation (Loucks, 1977). The shallow marine carbonates of the GRL from south of the study have documented hydrocarbon staining, but lacked significant structural or stratigraphic traps (Loucks, 1977). The hydrocarbon stainingdemonstrates the potential of karstic systems to act as reservoirs and ichnologic assessment may benefit such plays as the Edwards and Austin Chalk. This methodology may also be expanded into other potential reservoirs such as the Ellenburger Group of western TX

(Loucks, 1999) or the Arbuckle Group of Central Oklahoma (Kerans, 1988; Puckette et al., 2009).

Acknowledgments

The authors would like to recognize the landowners and managers of private and public lands in Bandera, Blanco, Bexar, Comal, Hays, and Kendall counties who provided access to their property for this study. We extend particular thanks to Ronald G. Fieseler, General Manager of the Blanco-Pedernales Groundwater Conservation District for his efforts in contacting various private land owners. We thank Stephen T. Hasiotis of the University of Kansas for his assistance with ichnofossil identification for this project. We would like to thank David V. Smith of the U.S. Geological Survey's USGS Crustal Geophysics and Geochemistry Science Center, for his supervision and leadership over the course of this project. We also thank the Kansas Interdisciplinary Carbonates Consortium for funding portions of this research. Finally, we thankboth of our reviewers for their insights that made this manuscript more effective.

7.0 References

Achauer, C.A., 1977, Contrasts in Cementation, Dissolution, and Porosity Development Between Two Lower Cretaceous Reefs of Texas, in Bebout, D.G., and Loucks, R.G., eds., Cretaceous carbonates of Texas and Mexico—Applications to subsurface exploration: Austin, University of Texas, Bureau of Economic Geology Report of Investigation 89, p. 127–137.

Adkins, W.S., 1928, Handbook of Texas Cretaceous Fossils: University of Texas Bulletin, no. 2838, 385 p.

Ashworth, J.B., 1983, Ground-water Availability of the Lower Cretaceous Formations in the Hill Country of South-central Texas: Texas Department of Water Resources Report 273, 172 p.

Babcock, L.E., Merriam, D.F., West, R.R., 2000, *Paleolimulus*, an Early Limuline (*Xiphosurida*), from Pennsylvanian–Permian Lagerstätten of Kansas and Taphonomic Comparison with Modern *Limulus*: Lethaia, vol. 33, p. 129–141.

Baniak, G.M., Gingras, M.K., and Pemberton, S.G., 2013, Reservoir Characterization of Burrow-Associated Dolomites in the Upper Devonian Wabamun Group, Pine Creek Gas Field, Central Alberta, Canada: Marine and Petroleum Geology, vol. 48, p. 275–292.

Barker, R.A., and Ardis, A.F., 1996, Hydrogeological Framework of the Edwards-Trinity Aquifer System, West-central Texas: U.S. Geological Survey Professional Paper 1421–B, 61 p.

Barnes, V.E., 1981, Geologic Atlas of Texas, Llano Sheet: Austin, University of Texas: Austin, Bureau of Economic Geology, 1 sheet, scale 1:250,000.

Barnes, V.E., 1965, Geology of the HaysQuadrangle, Blanco, Gillespie and Kendall Counties, Texas: Austin, University of Texas-Austin, Bureau of Economic Geology, 1 sheet, scale 1:24,000.

Bebout, D.G., Schatzinger, R.A., and Loucks, R.G., 1977, Porosity distribution in the Stuart City Trend, Lower Cretaceous, South Texas: in Bebout, D. G. and Loucks, R. G., eds., Cretaceous Carbonates of Texas and Mexico: Bureau of Economic Geology, University of Texas at Austin, Report of Investigations No. 89, p. 234–256.

Behrens, E.W., 1965, Environment Reconstruction for a Part of the Glen Rose Limestone, Central Texas: Sedimentology, vol. 4, p. 65–111.

Blome, C.D., and Clark, A.K., 2014, Key Subsurface Data Help to Refine Trinity Aquifer Hydrostratigraphic Units, South-central Texas: U.S. Geological Survey Data Series 768, 1 sheet, http://dx.doi.org/10.3133/ds768.

Blome, C.D., Faith, J.R., and Ozuna, G.B., 2007, Geohydrologic Framework of the Edwards and Trinity Aquifers, South-Central Texas: U.S. Geological Survey Fact Sheet 2006-3145, 4 p.

Braun, A.S., 2011, East to West Stratigraphic Cross Section, Northern Hays County: Surface to Subsurface Trinity Lithostratigraphy: in Implications for Groundwater Availability in the Hill Country, Eastern Blanco and Northern Hays Counties, Texas: Austin Geological Society, Guidebook 33.

Bromley, R.G., and Ekdale, A.A., 1986, Composite ichnofabrics and tiering of burrows: Geological Magazine, vol. 123, p. 59–65.

Bromley R.G. and Frey R.W., 1974, Redescription of the Trace Fossil *Gyrolithes* and Taxonomic Evaluation of *Thalassinoides*, *Ophiomorpha*, and *Spongeliomorpha*: Bulletin of the Geological Society of Denmark, vol. 23, p. 312–335.

Bumgarner, J.R., Stanton, G.P., Teeple, A.P., Thomas, J,V., Houston, N,A., Payne, J.D., Musgrove, M., 2012, A Conceptual Model of the Hydrogeologic Framework, Geochemistry, and Groundwater-flow System of the Edwards-Trinity and Related Aquifers in the Pecos County Region, Texas: SGS Scientific Investigations Report: 2012-5124, 74 p.

Carew, J.L., 1967, Study of a Portion of the Lower Glen Rose Formation, Steiner Ranch, Texas, in Scott, A.J. ed., Carbonate Depositional Environments, Central Texas, term reports: Department of Geology, Geology 383K, University of Texas, Austin, Texas, p. 54–63.

Choquette, P.W., and Pray, L.C., 1970, Geologic Nomenclature and Classification of Porosity in Sedimentary Carbonates: American Association of Petroleum Geologists Bulletin, vol. 54, no. 2, p. 207–250.

Clark, A.K., 2003, Geologic Framework and Hydrogeologic Features of the Glen Rose Limestone, Camp Bullis Training Site, Bexar County, Texas: U.S. Geological Survey Scientific Investigations Report 03–4081, 9 p., 1 pl., scale 1:24,000.

Clark, A.K., 2005, Geologic Framework and Hydrogeologic Characteristics of the Glen Rose Limestone, Camp Stanley Storage Activity, Bexar County, Texas: U.S. Geological Survey Scientific Investigations Map 2831, 1 pl., scale 1: 25,000.

Clark, A.K., Blome, C.D., and Morris, R.R., 2014, Geology and Hydrostratigraphy of Guadalupe River State Park and Honey Creek State Natural Area, Kendall and Comal Counties, Texas: U.S. Geological Survey Scientific Investigations Map 3303, 8 p., 1 sheet, scale 1:24,000.

Clark, A.K., Golab, J.A., and Morris, R.R., 2016, Geologic Framework, Hydrostratigraphy, and Ichnology of the Blanco, Payton, and Rough Hollow 7.5-minute Quadrangles, Blanco, Comal, Hays, and Kendall Counties, Texas: U.S. Geological Survey Scientific Investigations Map 3363, 21 p., 1 sheet, scale 1:24,000.

Clark, A.K., and Morris, R.R., 2015, Geologic and Hydrostratigraphic map of the Anhalt, Fischer, and Spring Branch 7.5-minute Quadrangles, Blanco, Comal, and Kendall Counties,

Texas: U.S. Geological Survey Scientific Investigations Map 3333, 13 p., 1 sheet, scale 1:50,000.

Clark, A.R., Blome, C.D., and Faith, J.R., 2009, Map Showing Geology and Hydrostratigraphy of the Edwards Aquifer Catchment Area, Northern Bexar County, South-Central Texas: U.S. Geological Survey Open-File Report 2009-1008.

Cleaves, A.W., 1977, Middle Glen Rose (Cretaceous) Facies Mosaic, Blanco and Hays Counties, Texas, in Bebout, D.G., and Loucks, R.G., eds., Cretaceous carbonates of Texas and Mexico—Applications to subsurface exploration: Austin, University of Texas, Bureau of Economic Geology Report of Investigation 89, 168 p.

Collins, E.W., 1992a, Geologic Map of the Anhalt 7.5-minute Quadrangle, Comal, Blanco, and Kendall Counties, Texas: The University of Texas at Austin, Bureau of Economic Geology Open-File Map OFM0095, 1 sheet, scale 1:24,000.

Collins, E.W., 1992b, Geologic Map of the Fischer 7.5-minute Quadrangle, Comal, Blanco, and Kendall Counties, Texas: The University of Texas at Austin, Bureau of Economic Geology Open-File Map OFM0030, 1 sheet, scale1:24,000.

Collins, E.W., 1992c, Geologic Map of the Spring Branch 7.5-minute Quadrangle, Comal, Blanco, and Kendall Counties, Texas: The University of Texas at Austin, Bureau of Economic Geology Open-File Map OFM0011, 1 sheet, scale 1:24,000.

Collins, E.W., 1995, Structural Framework of the Edwards Aquifer, Balcones Fault Zone, Central Texas: Gulf Coast Association of Geological Societies, Transactions, vol. 38, p. 135–141.

Conwy Valley Systems Ltd., 2011, PetrogLite Version 3.0 for MS Windows OS. Conway, United Kingdom.

Cunningham, K.J. and Sukop, M.C., 2011, Multiple Technologies Applied to Characterization of the Porosity and Permeability of the Biscayne Aquifer, Florida: U.S. Geological Survey Open-File Report 2011-1037, 8 p.

Cunningham, K.J. and Sukop, M.C., 2012, Megaporosity and Permeability of *Thalassinoides*-Dominated Ichnofabrics in the Createaceous Karst-Carbonate Edwards-Trinity Aquifer System, Texas: U.S. Geological Survey Open-File Report 2012-1021, 4 p.

Cunningham, K.J., Sukop, M.C., Huang, H., Alvarez, P.F., Curran, H.A., Renken, R.A., and Dixon, J.F., 2009, Prominence of Ichnologically Influenced Macroporosity in the Karst Biscayne aquifer: Stratiform “super-K” zones, Geological Society of America Bulletin, vol. 121, no. 1/2; p. 164–180.

Droser, M.J. and Bottjer, D.J., 1986, A Semiquantitative Field Classification of Ichnofabric: Journal of Sedimentary Petrology, vol. 56, no. 4, p. 558–559.

Dunham, R.J., 1962, Classification of Carbonate Rocks According to Depositional Textures: in American Association of Petroleum Geologists Memoir 1: Classification of Carbonate Rocks—A Symposium, p. 108–121.

Ekdale, A.A. and Bromley, R.G., 1984a, Comparative Ichnology of Shelf-Sea and Deep-Sea Chalk: Journal of Paleontology, vol. 58, p. 322–332.

Ekdale, A.A. and Bromley, R.G., 1984b, Sedimentology and Ichnology of the Cretaceous-Tertiary Boundary in Denmark: Implications for the Causes of the Terminal Cretaceous Extinction: Journal of Sedimentary Petrology, vol. 54, p. 681–703.

Embry, A.F. and Klovin, J.E., 1971, A Late Devionian Reef Bank on Northeastern Banks Island, N.W.T.: Bulletin of Canadian Petroleum Geology, vol. 19, no. 4, p. 730–781.

Faith, J.R., 2004, Strain and Fractures in an Extensional Relay Ramp, Sierra del Carmen, Black Gap Wildlife Management Area, Brewster County, Texas—Implications for Determining Structural Controls on Groundwater Flow Pathways in the Edwards Aquifer, South-central Texas: University of Texas at San Antonio, M.S. thesis, 88 p.

Fisher, W.L. and Rodda, P.U., 1969, Edwards Formation (Lower Cretaceous), Texas: Dolomitization in a Carbonate Platform System: American Association of Petroleum Geologists Bulletin, vol. 55, no. 1, p. 55–72.

Gary, M.O., Rucker, D.F., Smith, B.D., Smith, D.V., and Befus, K., 2013, Geophysical Investigations of the Edwards-Trinity Aquifer System at Multiple Scales: Interpreting Airborne and Direct-Current Resistivity in Karst: NCKRI Symposium 2, 13th Sinkhole Conference, p. 195–206.

George, W.O., 1952, Geology and Ground-water Resources of Comal County, Texas: U.S. Geological survey Water-Supply Paper 1138, 126 p.

Gingras, M.K., Baniak, G., Gordon, J., Hovikoski, J., Konhauser, K.O., LaCroix, A.D., Lemiski, R., Mendoza, C., Pemberton, S.G., Polo, C., and Zonneveld, J., 2012, Porosity and Permeability in Bioturbated Sediments: Developments in Sedimentology, vol. 64, p. 837–868.

Gingras, M.K., Pemberton, S.G., Mendoza, C.A., and Henk, F., 1999, Assessing the Anisotropic Permeability of *Glossifungites* Surfaces: Petroleum Geoscience, vol. 5, p. 349–357.

Gingras, M.K., Mendoza, C.A., and Pemberton, S.G., 2004, Fossilized Worm Burrows Influence the Reservoir Quality of Porous Media: American Association of Petroleum Geologists Bulletin, vol. 88, no. 7, p. 875–883.

Golab, J.A., Clark, A.K., and Hasiotis, S.T., 2015, Bioturbation-Influenced Fluid Pathways within a Carbonate Platform System: The Aptian–Albian Glen Rose Limestone: GSA Annual Meeting, Baltimore, MD, 1–4 November.

Grimshaw, T. W., and Woodruff Jr., C.M., 1986, Structural Style in an *En Echelon*Fault System, Balcones Fault Zone, Central Texas: Geomorphologic and Hydrologic Implications, in Abbott, P. L. and Woodruff, Jr., C.M., eds., The Balcones Escarpment—Geology, Hydrology, Ecology and Social Development in Central Texas: Guidebook published for the 1986 Geological Society of America Annual Meeting, San Antonio, Texas, p. 71–75.

Hanson, J.A., and Small, T.A., 1995, Geologic Framework and Hydrogeologic Characteristics of the Edwards Aquifer Outcrop, Hays County, Texas: U.S. Geological Survey Water-Resources Investigations Report 95–4265, 10 p.

Hasiotis, S.T. and Mitchell, C.E., 1993, A Comparison of Crayfish Burrow Morphologies: Triassic and Holocene Fossil, Paleo- and Neo-ichnological Evidence, and the Identification of Their Burrowing Signatures: Ichnos, vol. 2, p. 291–314.

Hasiotis, S.T. and Platt, B.R., 2012, Exploring the Sedimentary, Pedogenic, andHydrologic Factors that Control the Occurrenceand Role of Bioturbation in Soil Formation andHorizonation in Continental Deposits:An Integrative Approach: The Sedimentary Record, vol. 10, p.4–9.

Horvorka, S.D., Dutton, A.R., Ruppel, S.C., and Yeh, J., 1994, Sedimentologic and Diagenetic Controls on Aquifer Properties, Lower Cretaceous Edwards Carbonate Aquifer, Texas: Implications for Aquifer Management: Transactions of the Gulf Coast Association of Geological Societies, vol. 44, p. 277–284.

Hunt, B.B. and Smith, B.A., 2010, Spring 2009 Potentiometric Map of the Middle Trinity Aquifer in Groundwater Management Area 9, Central Texas: Barton Springs/Edwards Aquifer Conservation District Report of Investigations 2010-0501, 31 p.

Inden, R. F., 1974, Lithofacies and Depositional Model for a Trinity Cretaceous Sequence, Central Texas: in Aspects of Trinity Geology: Geoscience and Man, vol. 8, p. 37–52.

Imlay, R.W., 1945, Subsurface Lower Cretaceous Formations of South Texas: American Association of Petroleum GeologistsBulletin, vol. 29, p. 1416–1469.

Kerans, C., 1988, Karst-controlled Reservoir Heterogeneity in Ellenburger Group Carbonates of West Texas: American Association of Petroleum Geologists Bulletin, vol. 72, no. 10, p. 1160–1183.

Keswani, A. D. and Pemberton, S. G., 2007, Applications of Ichnology in Exploration and Exploitation of Mississippian Carbonate Reservoirs, Midale Beds, Weyburn Oilfield, Saskatchewan. In Alberta, Canada, Canadian Society of Petroleum Geologists and Canadian Society of Exploration Geophysicists Conference, p. 14–17.

Kraus, M. J. and Hasiotis, S.T., 2006, Significance of Different Modes of Rhizolith Preservation to Interpreting Paleoenvironmental and Paleohydrologic Settings: Examples from Paleogene Paleosols, Bighorn Basin, Wyoming, U.S.A.: Journal of Sedimentary Research, vol. 76, no. 4,p. 633–646.

La Croix, A.D., Gingras, M.K., Dashtgard, S.E., and Pemberton, S.G., 2012, Computer Modeling Bioturbation: The Creation of Porous and Permeable Fluid-Flow Pathways: American Association of Petroleum GeologistsBulletin, vol. 96, no. 3, p. 545–556.

Loucks, R.G., 1977, Porosity Development and Distribution in Shoal-Water Carbonate Complexes—Subsurface Pearsall Formation (Lower Cretaceous) South Texas, in Bebout, D.G. and Loucks, R.G., eds., Cretaceous carbonates of Texas and Mexico—Applications to subsurface exploration: University of Texas at Austin, Bureau of Economic Geology Report of Investigation 89, p. 97–126.

Loucks, R.G., 1999, Paleocave Carbonate Reservoirs: Origins, Burial-Depth Modifications, Spatial Complexity, and Reservoir Implications: American Association of Petroleum Geologists Bulletin, vol. 83, no. 11, p. 1795–1834.

Lozo, F.E., and Stricklin Jr., F.L., 1956, Stratigraphic Notes on the Outcrop Basal Cretaceous, Central Texas: Gulf Coast Association of Geological Societies Transactions, vol. 6, p. 67–78.

Mace, R.E., Chowdhury, A.H., Anaya, H., Way, S., 2000, Groundwater Availability of the Trinity Aquifer, Hill Country Area, Texas: Numerical Simulations through 2050: Texas Water Development Board Report 353, 117 p.

Maclay, R.W., 1989, Edwards Aquifer in the San Antonio Region: Its Hydrology and Management: South Texas Geological Society Bulletin, vol. 30, no. 4, p. 11–28.

Maclay, R.W., 1995, Geology and Hydrology of the Edwards Aquifer in the San Antonio Area, Texas: U.S. Geological Survey Water Resources Investigations Report 95-4186, 64 p.

Maclay, R.W., and Small, T.A., 1976, Progress Report on Geology of the Edwards Aquifer, San Antonio Area, Texas, and Preliminary Interpretation of Borehole Geophysical and Laboratory Data on Carbonate Rocks: U.S. Geological Survey Open-File Report 76–627, 65 p.

Maclay, R.W., and Small, T.A., 1986, Carbonate Geology and Hydrology of the Edwards Aquifer in the San Antonio Area, Texas: Texas Water Development Board, Report 296, p. 90.

Mancini, E.A. and Scott, R.W., 2006, Sequence Stratigraphy of Comanchean Cretaceous Outcrop Strata of Northeast and South-Central Texas: Implications for Enhanced Petroleum Exploration: Gulf Coast Association of Geological Societies Transactions, vol. 56, p. 539–550.

Maxey, G.B., 1964, Hydrostratigraphic Units: Journal of Hydrology, vol. 2, p. 124–129.

Mazzullo, S.J. and Chilingarian, G.V., 1996, Hydrocarbon Reservoirs in Karsted Carbonate Rocks: Developments in Petroleum Science, vol. 44, no. 2, p. 797–865.

Mylroie, J.E. and Carew, J.L., 1990, The Flank Margin Model for Dissolution Cave Development in Carbonate Platforms: Earth Surface Processes and Landforms, vol. 15, p. 413–424.

Myrow, P.M., 1995, *Thalassinoides* and the Enigma of Early Paleozoic Open-Framework Burrow Systems: PALAIOS, vol. 10, no. 1, p. 58–74.

Pantea, M.P., Blome, C.D., and Clark, A.K. 2014, Three-Dimensional Model of the Hydrostratigraphy and Structure in and around the U.S. Army–Camp Stanley Storage Activity Area, Northern Bexar County, Texas: USGS Scientific Investigations Report 2014–5074.

Pantea, M.P., Cole, J.C., Smith, B.D., Faith, J.R., and Blome, C.D., 2008, Three-Dimensional Geologic Model of Complex Fault Structures in the Upper Seco Creek Area, Medina and Uvalde Counties, South-Central Texas: U.S. Geological Survey Scientific Investigations Report 2008–5131, DVD-ROM, 9 p.

Pemberton, S.G. and Frey, R.W., 1982, Trace Fossil Nomenclature and the *Planolites-Palaeophycus* Dilemma: Journal of Paleontology, vol. 56, no. 4, p. 843–881.

Perkins, B.F., 1974, Paleoecology of a Rudist Reef Complex in the Comanche Cretaceous, Glen Rose Limestone, Central Texas, in Perkins, B.F., ed., Aspects of Trinity Division Geology—A Symposium: Louisiana State University: Geoscience and Man, vol. 8, p. 131–173.

Petta, T.J., 1977, Diagenesis and geochemistry of a Glen Rose patch reef complex, Bandera County, Texas, in Bebout, D.G., and Loucks, R.G., eds., Cretaceous carbonates of Texas and Mexico—Applications to subsurface exploration: University of Texas at Austin, Bureau of Economic Geology Report of Investigation 89, p. 138–165.

Pittman, J.G., 1989, Stratigraphy of the Glen Rose Formation, Western Gulf Coast Plain: Gulf Coast Associations of Geological Societies Transactions, vol. 39, p. 247–264.

Puckette, J., Halihan, T., and Faith, J.R., 2009, Characterization of the Arbuckle-Simpson Aquifer—Final Report for the Arbuckle-Simpson Hydrology Study: Sillwater, Oklahoma, Oklahoma State University, School of Geology, for theOklahoma Water Resources Board, 53 p.

Riding, R., 2007, *Girvanella* and Other Algae as Depth Indicators: Lethaia, vol. 8, p. 173–179.

von Roemer, C.F., 1852, Die Kreidebildungen von Texas und Ihre Organischen Einschliisse: Bonn, p. 1–10.

Rose, P.R., 1972, Edwards Group, Surface and Subsurface, Central Texas: University of Texas at Austin, Bureau of Economic Geology Report of Investigations 74, 198 p.

Schlager,W., 1989, Drowning Unconformities on Carbonate Platforms: Controls on Carbonate Platform and Basin Development, SEPM Special Publication No. 44, p. 15–25.

Scanlon, B.R., Mace, R.E., Barrett, M.E., and Smith, B., 2003, Can We Simulate Regional Groundwater Flow in a Karst System Using Equivalent Porous Media Models? Case study, Barton Springs Edwards aquifer, USA: Journal of Hydrology, vol. 276, p.137–158.

Scott, R.W., Molineux, A.M., and Mancini, E.A., 2007, Lower Albian Sequence Stratigraphy and Coral Buildups—Glen Rose Formation, Texas, USA, in Scott, R.W., ed., Cretaceous Rudists and Carbonate Platforms—Environmental feedback: Society for Sedimentary Geology, v. 87, p. 181–191.

Sheehan, P.M. and Schiefelbein, D.R.J., 1984, The Trace Fossil *Thalassinoides* from the Upper Ordovician of the Eastern Great Basin: Deep Burrowing in the Early Paleozoic: Journal of Paleontology, vol. 58, no. 2, p. 440–447.

Small, T.A. and Lambert, R.B., 1998, Geologic Framework and Hydrogeologic Characteristics of the Outcrops of the Edwards and Trinity Aquifers, Medina Lake Area, Texas: U.S. Geological Survey Water-Resources Investigations Report 97–4290, 21 p.

Smith, B.D., Cain, M.J., Clark, A.K., Moore, D.W., Faith, J.R., Hill, P.R., 2005, Helicopter Electromagnetic and Magnetic Survey Data and Maps, Northern Bexar County, Texas: U.S. Geological Survey Open-File Report 05-1158, 24 p.

Smith, J.J., Hasiotis, S.T., Kraus, M.J., and Woody, D.T., 2008, Relationship of Floodplain Ichnocoenoses to Paleopedology, Paleohydrology, and Paleoclimate in the Willwood Formation, Wyoming, During the Paleocene–Eocene Thermal Maximum: PALAIOS, vol. 23, p. 683–699.

Stricklin, F. L. and Amsbury, D.L., 1974, Depositional Environments on a Low-Relief Carbonate Shelf, Middle Glen Rose limestone, Central Texas: Geoscience and Man, vol. 8, p. 53–66.

Stricklin, F.L., Jr., Smith, C.I., and Lozo, F.E., 1971, Stratigraphy of Lower Cretaceous Trinity Deposits of Central Texas: University of Texas at Austin, Bureau of Economic Geology Report of Investigations 71, 63 p.

Tonkin, N.S., McIlroy, D., Meyer, R., and Moore-Turpin, A., 2010, Bioturbation Influence on Reservoir Quality: A Case Study from the Cretaceous Ben Nevis Formation, Jeanne d'Arc

Basin, Offshore Newfoundland, Canada: American Association of Petroleum GeologistsBulletin, vol. 94, p. 1059–1078.

Uchman, A., 1995, Taxonomy and Palaeoecology of Flysch Trace Fossils: The Marnosoarenacea Formation and Associated Facies (Miocene, Northern Apennines, Italy): Beringeria, vol. 15, p. 3.

Uchman, A., 1998, Taxonomy and Ethology of Flysch Trace Fossils: ARevision of the Marian-Książkiewicz Collection and Studies of Complementary Material: Annales Societatis Geologorum Poloniae, vol. 68, p. 105–218.

Vinn, O., Hove, H.A.T., Mutvei, H., and Kirsimäe, K., 2008, Ultrastructure and Mineral Composition of Serpulid Tubes (Polychaeta, Annelida): Zoological Journal of the Linnean Society, vol. 154, p. 633–650.

Ward, W.C. and Ward, B.W., 2007, Stratigraphy of Middle Part of the Glen Rose Formation (Lower Albian), Canyon Lake Gorge, Central Texas, U.S.A.: Cretaceous Rudists and Carbonate Platforms: Environmental Feedback: SEPM Special Publication 87, p. 193–210.

Wentworth, C.K., 1922, A Scale of Grade and Class Terms for Clastic Sediments: Journal of Geology, vol. 31, p. 377–392.

Whitney, M.I., 1952, Some Zone Marker Fossils of the Glen Rose Formation of Central Texas: Journal of Paleontology, vol. 26, no. 1, p. 65–73.

Winter, J.A., 1961, Stratigraphy of the Lower Cretaceous (Subsurface) of South Texas: Gulf Coast Association of Geological Societies Transactions, vol. 11, p.15–24.

Winters, W.J., Dallimore, S.R., Collett, T.S., Katsube, T.J., Jenner, K.A., Cranston, R.E., Wright, J.F., Nixon, F.M., and Uchida, T., 1999, Physical Properties of Sediments from the JAPEX/JNOC/GSC Mallik 2L-38 Gas Hydrate Research Well: in Dallimore, S.R., Uchida, T., and Collett, T.S., eds., Scientific Results from JAPEX/JNOC/GSC Mallik 2L-38 Gas Hydrate Research Well, Mackenzie Delta, Northwest Territories, Canada: Geological Survey of Canada Bulletin 544, p. 95–100.

Wright, V.P., Baceta, J.I., Lapointe, P.A., 2014, Paleokarstic Macroporosity Development at Platform Margins: Lessons from the Paleocene of North Spain: Interpretation, vol. 2, p. 1–16.

Zhou, W., Beck, B.F., Adams, A.L., 2002, Effective Electrode Array in Mapping Karst Hazards in Electrical Resistivity Tomography: Environmental Geology, vol. 42, p. 922–928.

8.0 Captions

Figures

Figure 1. Location map showing the regional extent of the Edwards and Trinity aquifer outcrop and subsurface catchment area as well as the extent of carbonate platform deposition in Texas. Locations of the Llano Uplift and Stuart City Reef, which affected GRL deposition, are also shown. Approximate locations of the four measured sections and two cores used in this study are indicated. Regional aquifer extent modified from Blome et al. (2007); extent of carbonate deposition and location of regional features modified from Pittman (1989).

Figure 2. Chart summarizing the lithostratigraphy, sequence stratigraphy, and hydrostratigraphy of the Trinity Group on the Central Texas Platform. Hosston and Sligo formations are found only in the subsurface within the study area. The Pearsall Formation and Glen Rose Limestone were examined in outcrop and core. The overlying Edwards Group is found in some outcrops within the study area. Ages of formations and members from Stricklin et al. (1971) and Clark and Morris (2015).

Figure 3. Lithofacies of the Glen Rose Limestone within the study area. A) Weathered outcrop section of nodular and massive marly fossiliferous wackestone–packstone. B) Roadcut section showing a detailed, unweathered face of nodular and massive marly fossiliferous wackestone–packstone. C) Outcrop of bedded and crossbedded argillaceousfossiliferous wackestone–packstone with low-angle crossbedding. D) Close-up photograph of bedded and crossbedded argillaceousfossiliferous wackestone–packstone showing low angle crossbedding. E) Outcrop of

well indurated, ledge-forming fossiliferous grainstone (arrow) with a sharp basal contact above a nodular, marly fossiliferous wackestone–packstone.

Figure 4. Lithofacies of the Glen Rose Limestone within the study area(continued). A) Weathered outcrop of boxwork gypsum and mudstone within evaporitic mudstone facies. B) Symmetrical ripples in *Corbula* packstone–grainstone facies. Top of bed shown in photograph is the contact between the Upper and Lower Glen Rose Limestone. C) Close-up photograph of *Corbula* packstone–grainstone facies showing detailed *Eoursivivas harveyi* shells. D) *Caprinid* sp. in life position within rudist-dominated bafflestone facies. E) Laminated calcareous mudstone in core MW6-LGR with convoluted laminae (arrows). F) Carbonate-cemented sandstone with brecciated limestone clasts (arrows).

Figure 5. Ichnofossils of the Glen Rose Limestone within the study area. A)*Thalassinoides* network with packstone infill dominated by skeletal grains of the foraminfera *Orbitolina texana.* Matrix around the burrows has been weathered out following exposure, but was originally mudstone.B) Solution-enhanced *Thalassinoides* network with packstone infill within a wackestone matrix (arrows). Packstone infill is fossiliferous and similar to overlying wackestone–packstone strata. C) *Thalassinoides* network with solution-enhanced open burrows throughout the strata. D) *Palaeophycus*with packstone infill and a distinct, brown-tan oxidized mud lining. Found in association with *Thalassinoides* networks. E) *Planolites* with distinct, light-colored mudstone infill oriented parallel to bedding surface within a wackstone matrix. F) *Planolites* with distinct, light-colored mudstone infill (arrow) within a conglomeratic matrix containing detrital clasts.

Figure 6. Ichnofossils of the Glen Rose Limestone within the study area. A) *Ophiomorpha* within a packstone matrix with similar packstone infill. Pellets are visible around the burrow (arrow) B) *Ophiomorpha*with branching networks and weathered-out matrix due to subaerial exposure. C)Serpulid tube on a bivalve shell showing typical coiled morphology. D) Thin-section pictomicrograph of a serpulid tube from core MW9-CC showing cement coating and laminated mud infill. Growth of sparry cement acts as a geopetal (arrow). E) Rhizolith and rhizohalo within a highly bioturbated (ii5) marly wacketone. F) Spherical rhizocretions formed around roots and root hairs indicating abundant plant growth during subaerial exposure (arrows). G) *Cruziana* oriented along a bedding surface and indicating firmground–hardground conditions. This *Cruziana* is ~13.0 cm wide and ~59.3 cm long; lens cap is 5.7 cm in diameter.

Figure 7. Model of ichnofabric index (ii) progression in *Thalassinoides*-dominated Glen Rose Limestone strata based on the scheme of Droser and Bottjer (1986). A) Top shows a single bed with ii2 and *Palaeophycus* and bottom shows the development of an untiered *Thalassinoides* network with ii3. B) Bed with ii4 and interconnected*Thalassinoides* network. C) Further development of a tiered *Thalassinoides* network over time leading to ii5 and nodular bedding. D) Further development of *Thalassinoides* networks leading to completely homogenized sediment with ii6.

Figure 8. Chart showing overall dataset for the Glen Rose Limestone within the study area including: composite stratigraphic section, porosity and permeability data from He-expansion testing, matrix porosity from point counted data. Hydrostratigraphic units are designated as either

transmissive (T) or confining (C) according to Clark (2003) and Clark and Morris (2015). Porosity and permeability data from He-expansion testing in Lower Glen Rose Limestone core MW5-LGR modified from Blome and Clark (2014). Uppermost Cavernous hydrostratigraphic unit not shown on column as it is not present in outcrop within the study area.

Figure 9. Stratigraphic column from the Lower Glen Rose Limestone (GRL) Honey Creek hydrostratigraphic unit in Hays County, Texas showing the typical coarsening-upward successions and ichnofabric index (ii) patterns seen in Lower GRL transmissive units. Interpretations of fluid-flow characteristics shown under Hydrostratigraphy.

Figure 10. Stratigraphic column from the Lower Glen Rose Limestone (GRL) Twin Sisters hydrostratigraphic unit from core in northern Blanco County, Texas showing the typical marly sedimentation and ichnofabric index (ii) patterns seen in Lower GRL confining units. Interpretations of fluid-flow characteristics shownunder Hydrostratigraphy.

Figure 11. Stratigraphic column from the Upper Glen Rose Limestone (GRL) Camp Bullis hydrostratigraphic unit (HSU) in Kendall County, Texas showing the typical coarsening-upward successions and ichnofabric index (ii) patterns seen in Upper GRL confining units. These units have been described in this report as “semi-confining”.Interpretations of fluid-flow characteristics shownunder Hydrostratigraphy.

Figure 12. Diagram showing the progression of solution enhancement within the GRL. T_1) The initial condition of coarse-grained infilled Thalassinoides (Th) and Palaeophycus (Pa). T_2)

Introduction of meteoric water begins to dissolve the matrix surrounding the burrows and dissolve infill. T_3) Dissolution of matrix material interconnects burrow networks across the three-dimensional extent of the bed. T_{4a}) Solution-enhanced burrow networks filled with sediment being moved by groundwater flow and cemented. T_{4b}) Cemented, solution-enhanced burrows weather differentially from the surrounding matrix and are preserved in positive relief. T_{5b}) Continued dissolution of matrix surrounding burrows from meteoric water thins rock between networks. T_{5b}) Weight of overburden collapses strata and creates a brecciated bed.

Table 1

Lithofacies Code	Lithofacies Name	Lithology and Sedimentary Structures	Thickness	Porosity	Ichnofossils
Nwp	Nodular and massive marly wackestone–packstone (Figs. 3A–B)	Gray–tan, wackestone–packstone containing mostly shell fragment clasts. Clasts include foraminiferans, gastropods, bivalves, mollusks, and echinoid shells. Few sedimentary structures present. Appears nodular in outcrop.	0.1–1.8 m	Fracture, moldic, and shelter. 8–35% matrix porosity.	*Thalassinoides* , *Ophiomorpha* , *Palaeophycus* , *Planolites* , rhizoliths, Serpulid tubes
Cwp	Cross-bedded argillaceous wackestone–packstone (Figs. 3C–D)	Gray, argillaceous wackestone–packstone containing whole and very fine- to medium-grained fragmentary shell clasts. Shells include gastropod, bivalve, mollusk, and echinoid shells. Contains low-angle trough cross-beds and some laminations. Iron staining and dendrites are common.	0.2–0.4 m	Biotutbation-influenced, fracture, moldic, shelter, fenestral, and interparticle. 8–23% matrix porosity.	*Thalassinoides* , *Ophiomorpha* , *Palaeophycus* , *Planolites*, rhizoliths, Serpulid tubes, *Cruziana*
Fgs	Fossiliferous grainstone (Fig. 3E)	Gray–tan, grainstone consisting of shell fragments and submarine calcite cement. Clasts include gastropod, and echinoid shell fragments. Commonly massive, but some beds contain low-angle to trough crossbedding. Dendrites and pervasive iron staining are common.	0.5–1.3 m	Intergranular and fracture. 3–35% matrix porosity.	None
Ems	Evaporitic mudstone (Fig. 4A)	Gray–tan, carbonate mudstone with boxwork crystalline gypsum and anhydrite.Clasts rare, but contains some bivalve, gastropod, and echinoid shell fragments and whole *Orbitolina minuta* . Little to no primary sedimentary structures. Commonly massive and convoluted.	< 1 m	Fracture and moldic. 14–22% matrix porosity.	*Planolites*

Table 2

Hydrostratigraphic Unit	Lithofacies	Ichnofossils	Transimissivity	Bioturbation-influenced
Cavernous	Nwp	*Thalassinoides*	Transmissive	High
Camp Bullis	Nwp, Fgs, Lcm	*Thalassinoides* , *Ophiomorpha* , *Palaeophycus* , rhizoliths	Semi-confining	High
Upper Evaporite	Ems	*Planolities*	Transmissive	Very low
Fossiliferous	Nwp, Lcm, Rdf, Rdb	*Thalassinoides* , *Ophiomorpha* , *Palaeophycus* , rhizoliths, Serpulid tubes	Semi-confining	High
Lower Evaporite	Ems	*Planolities*	Transmissive	Very low
Bulverde	Nwp, Cwp, Cpg, Lcm, Rdf, Rdb	*Thalassinoides* , *Palaeophycus* , *Planolites* , *Cruziana* , rhizoliths	Semi-confining	Moderate
Little Blanco	Nwp, Cwp, Rdf, Rdb	*Thalassinoides* , *Palaeophycus* , *Planolites* ,	Transmissive	High
Twin Sisters	Nwp, Rdf, Rdb	*Thalassinoides*	Confining	Low
Doeppenschmidt	Nwp, Lcm, Rdf, Rdb	*Thalassinoides* , *Palaeophycus*	Transmissive	High
Rust	Nwp, Rdf, Rdb	*Thalassinoides* , *Palaeophycus* , *Planolites* ,	Confining	Low
Honey Creek	Nwp, Lcm, Rdf, Rdb, Ccs	*Thalassinoides* , *Palaeophycus* , *Planolites*	Transmissive	High

Figure 1

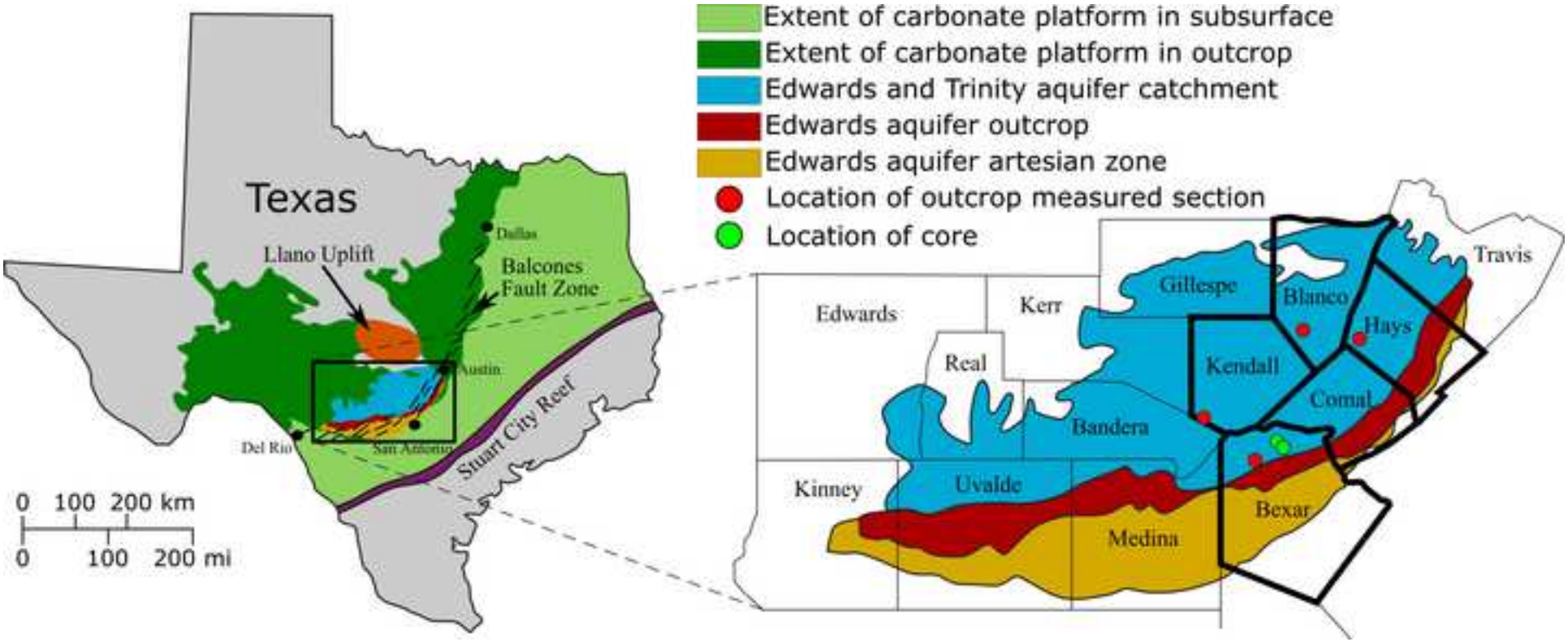
Extent of carbonate platform in subsurface
Extent of carbonate platform in outcrop
Edwards and Trinity aquifer catchment
Edwards aquifer outcrop
Edwards aquifer artesian zone
Location of outcrop measured section
Location of core
Texas
Llano Uplift
Balcones Fault Zone
Dallas
Austin
San Antonio
Del Rio
Stuart City Reef
0 100 200 km
0 100 200 mi
Edwards
Kerr
Real
Gillespe
Blanco
Hays
Travis
Kendall
Comal
Bandera
Kinney
Uvalde
Medina
Bexar

Figure 2

Epoch	Age	Group	Formation	Member	Sequence Stratigraphy	Hydrostratigraphic unit	Aquifer
Lower Cretaceous	Albian	Edwards	Kainer	Basal Nodular		VIII	Edwards
		Trinity	Glen Rose Limestone	Upper Glen Rose Limestone	Highstand Carbonate	Cavernous *Transmissive*	Upper Trinity
						Camp Bullis *Semi-confining*	
						Upper Evaporite *Transmissive*	
						Fossiliferous *Semi-confining*	
						Lower Evaporite *Transmissive*	
	Aptian			Lower Glen Rose Limestone		Bulverde *Semi-confining*	Middle Trinity
						Little Blanco *Transmissive*	
						Twin Sisters *Confining*	
						Doeppenschmidt *Transmissive*	
						Rust *Confining*	
						Honey Creek *Transmissive*	
			Pearsall	Hensell Sand	Lowstand Siliciclastic	Hensell *Confining*	
				Cow Creek Limestone	Highstand Carbonate	Cow Creek *Transmissive*	
				Hammett Shale	Lowstand Siliciclastic	Hammett *Confining*	Confining unit
			Sligo		Highstand Carbonate		Lower Trinity
	Barremian		Hosston		Lowstand Siliciclastic		
	Hauterivian						

Figure 3

Figure 4

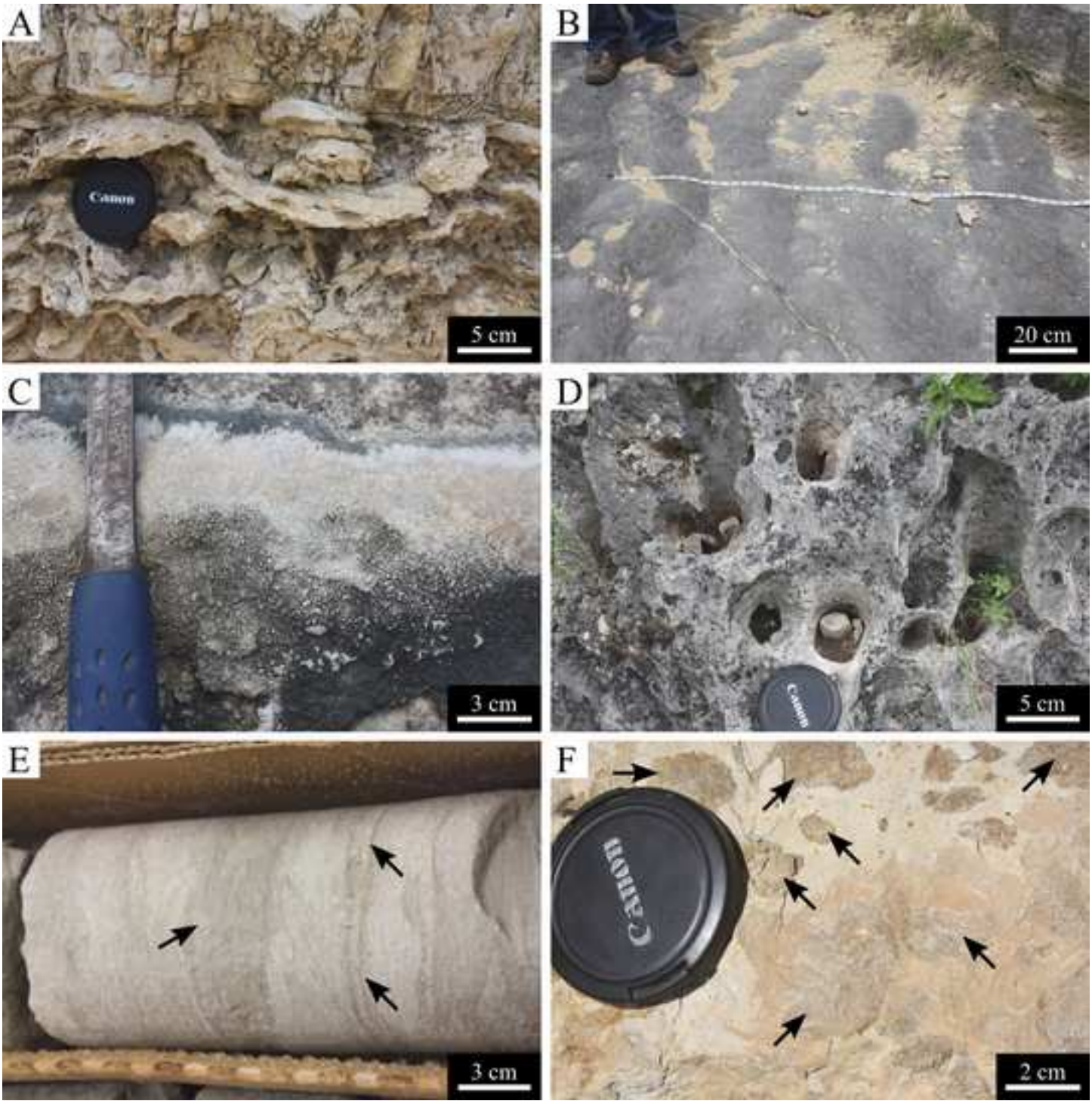

Figure 5

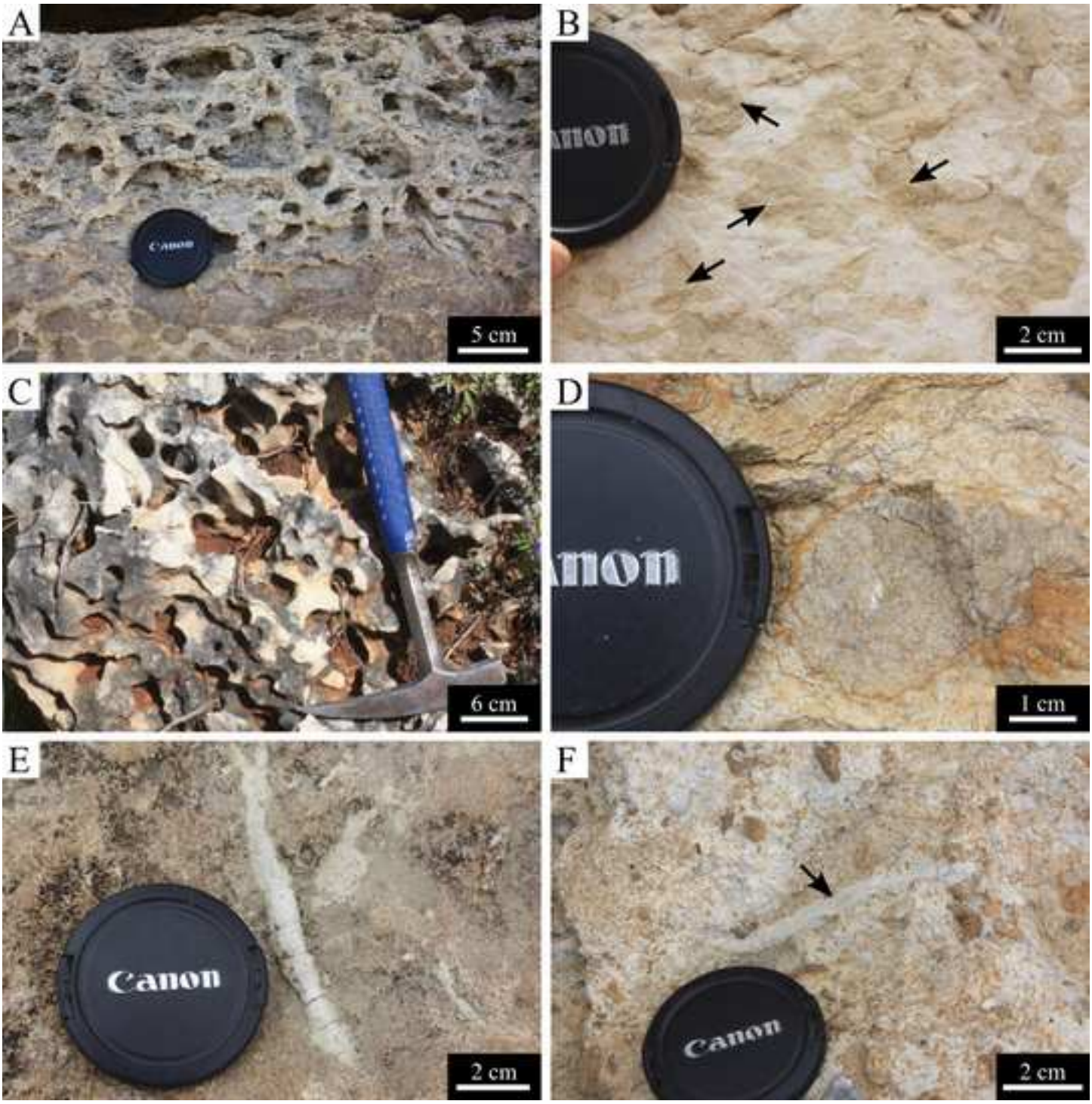

Figure 6

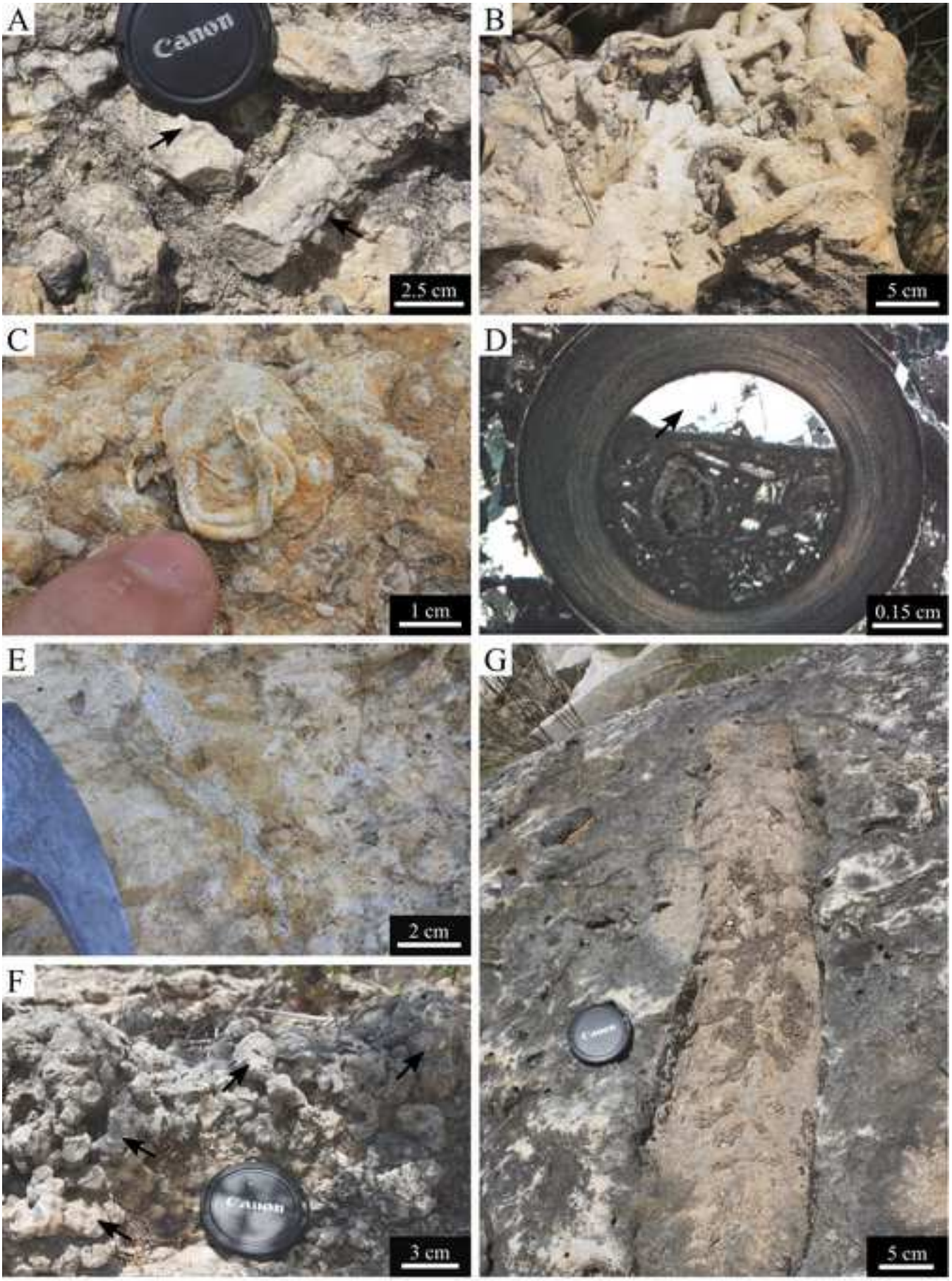

Figure 7

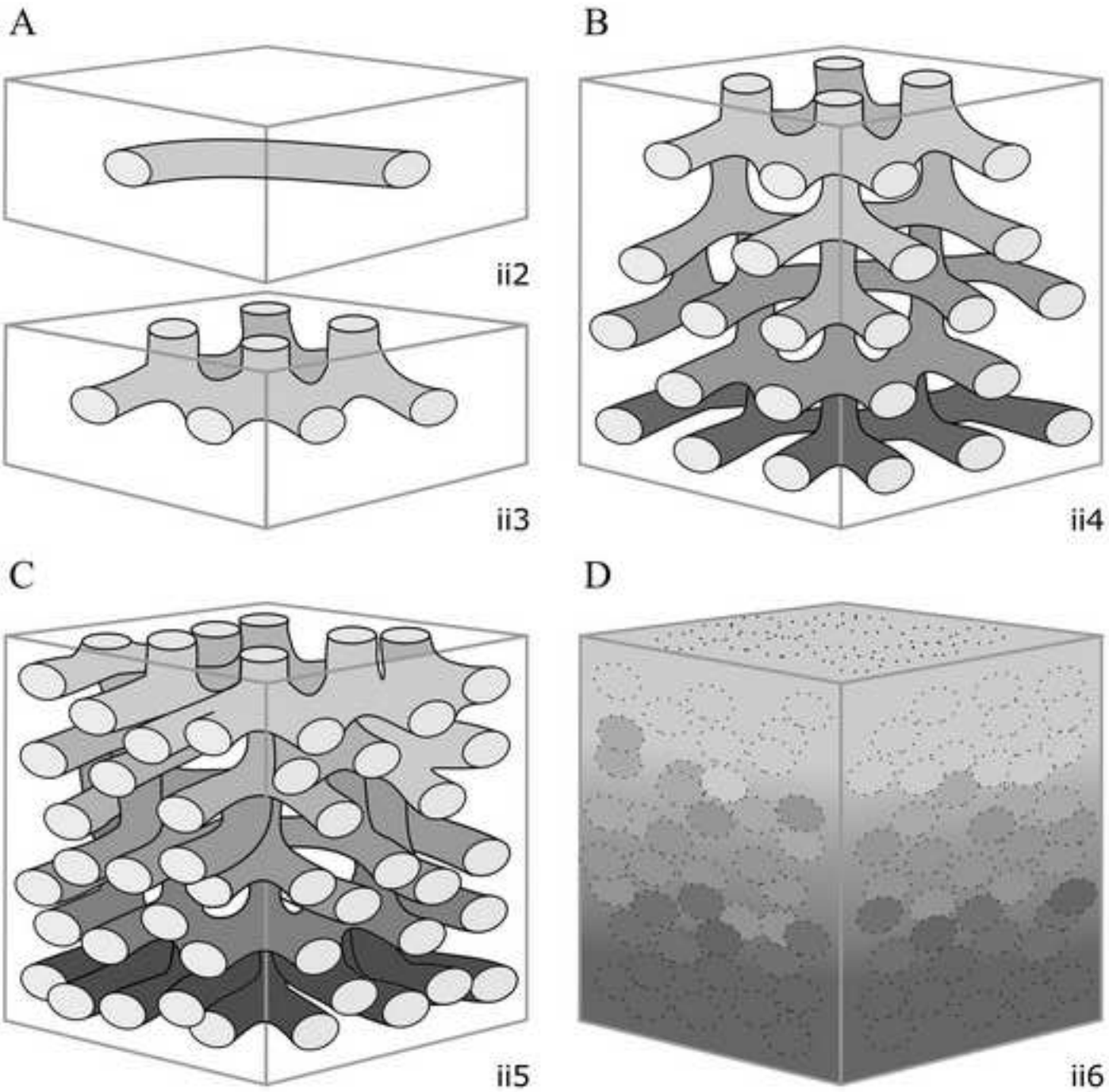

Figure 8

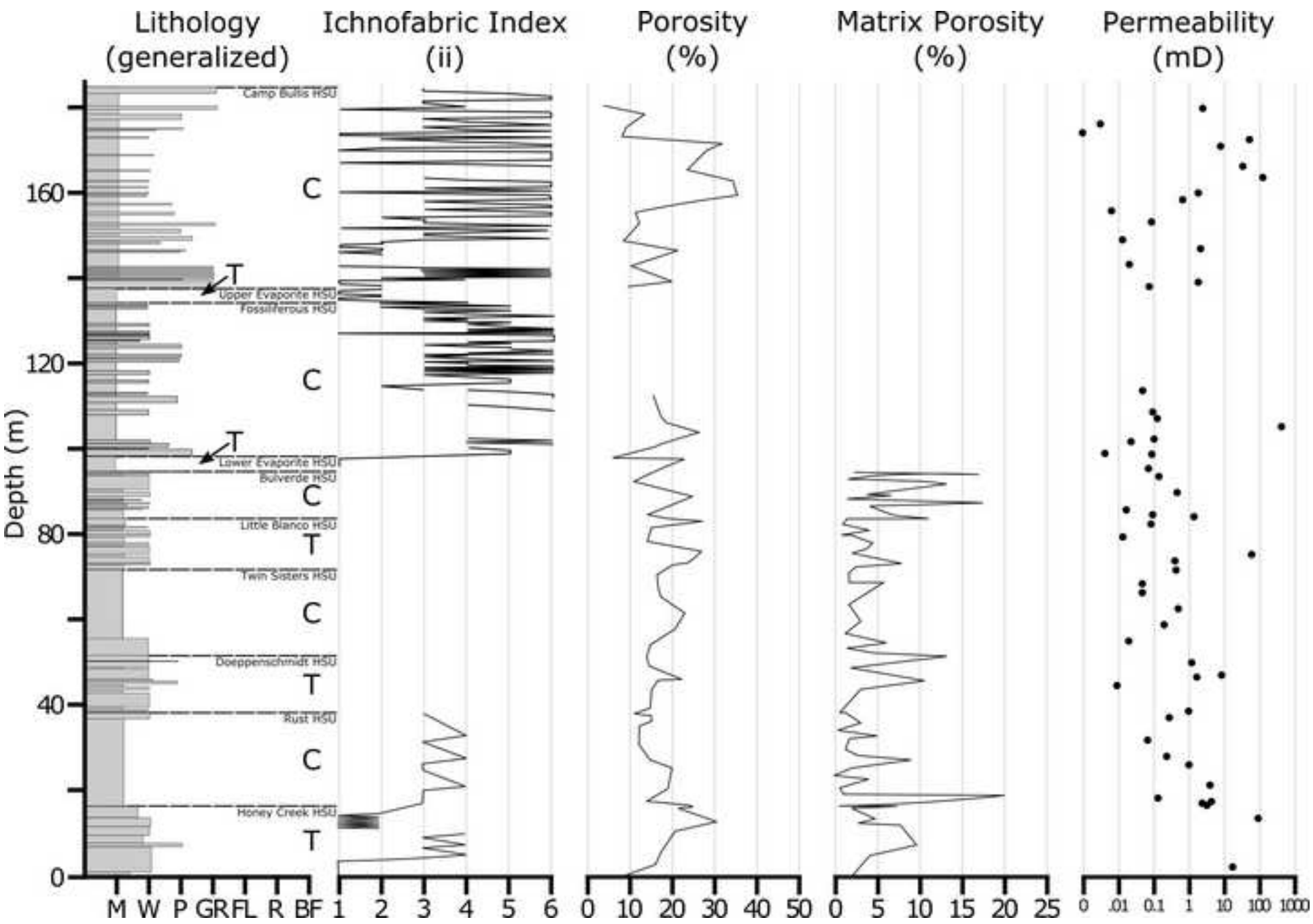
Lithology (generalized)
Ichnofabric Index (ii)
Porosity (%)
Matrix Porosity (%)
Permeability (mD)
Depth (m)
Camp Bullis HSU
Upper Evaporite HSU
Fossiliferous HSU
Lower Evaporite HSU
Bulverde HSU
Little Blanco HSU
Twin Sisters HSU
Doeppenschmidt HSU
Rust HSU
Honey Creek HSU
C
T
M W P GR FL R BF
1 2 3 4 5 6
0 10 20 30 40 50
0 5 10 15 20 25
0 .01 0.1 1 10 100 1000
0 40 80 120 160

Figure 9

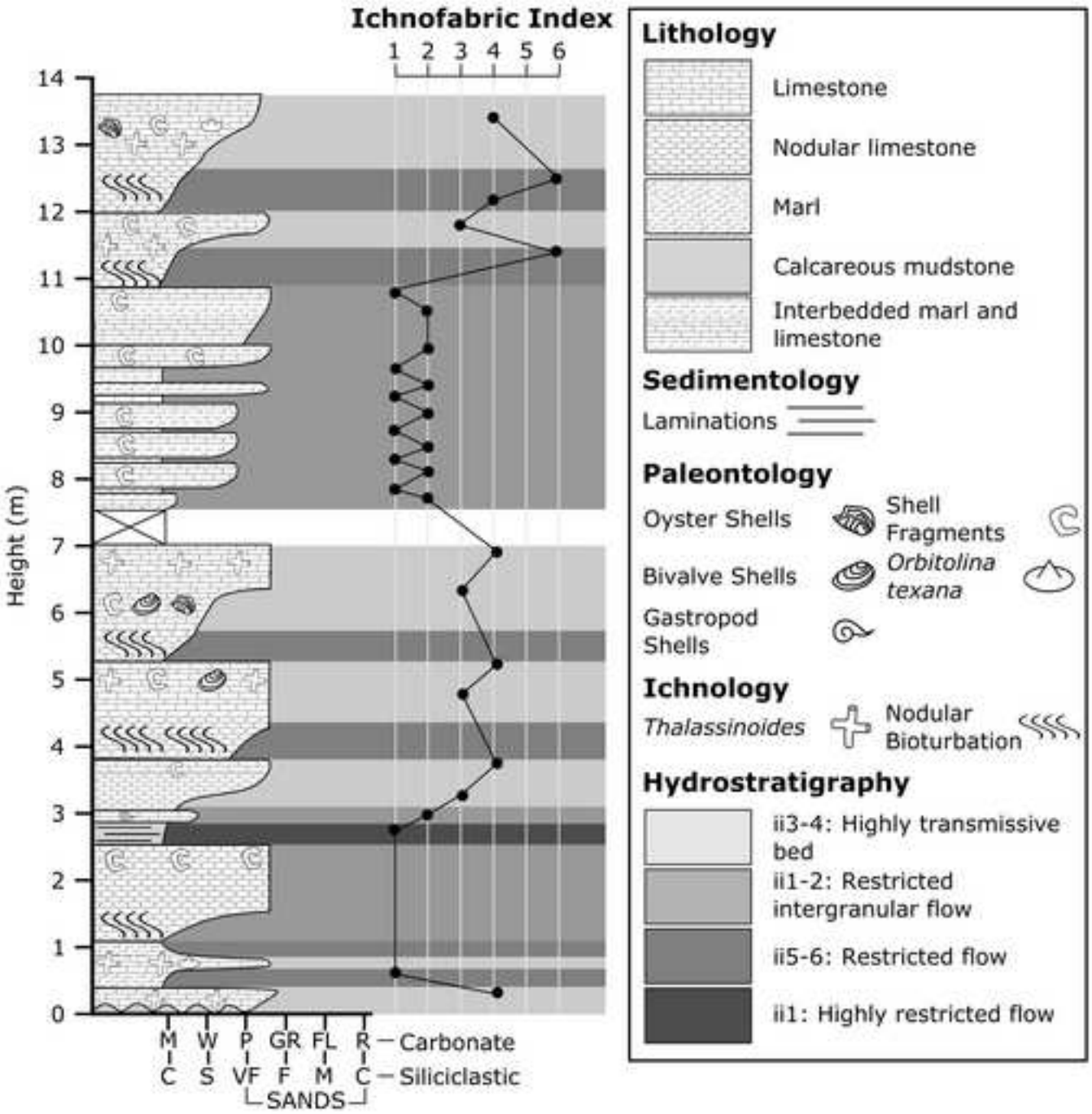
Ichnofabric Index
1 2 3 4 5 6
Height (m)
0 1 2 3 4 5 6 7 8 9 10 11 12 13 14
M W P GR FL R — Carbonate
C S VF F M C — Siliciclastic
SANDS
Lithology
Limestone
Nodular limestone
Marl
Calcareous mudstone
Interbedded marl and limestone
Sedimentology
Laminations
Paleontology
Oyster Shells
Shell Fragments
Bivalve Shells
Orbitolina texana
Gastropod Shells
Ichnology
Thalassinoides
Nodular Bioturbation
Hydrostratigraphy
ii3-4: Highly transmissive bed
ii1-2: Restricted intergranular flow
ii5-6: Restricted flow
ii1: Highly restricted flow

Figure 10

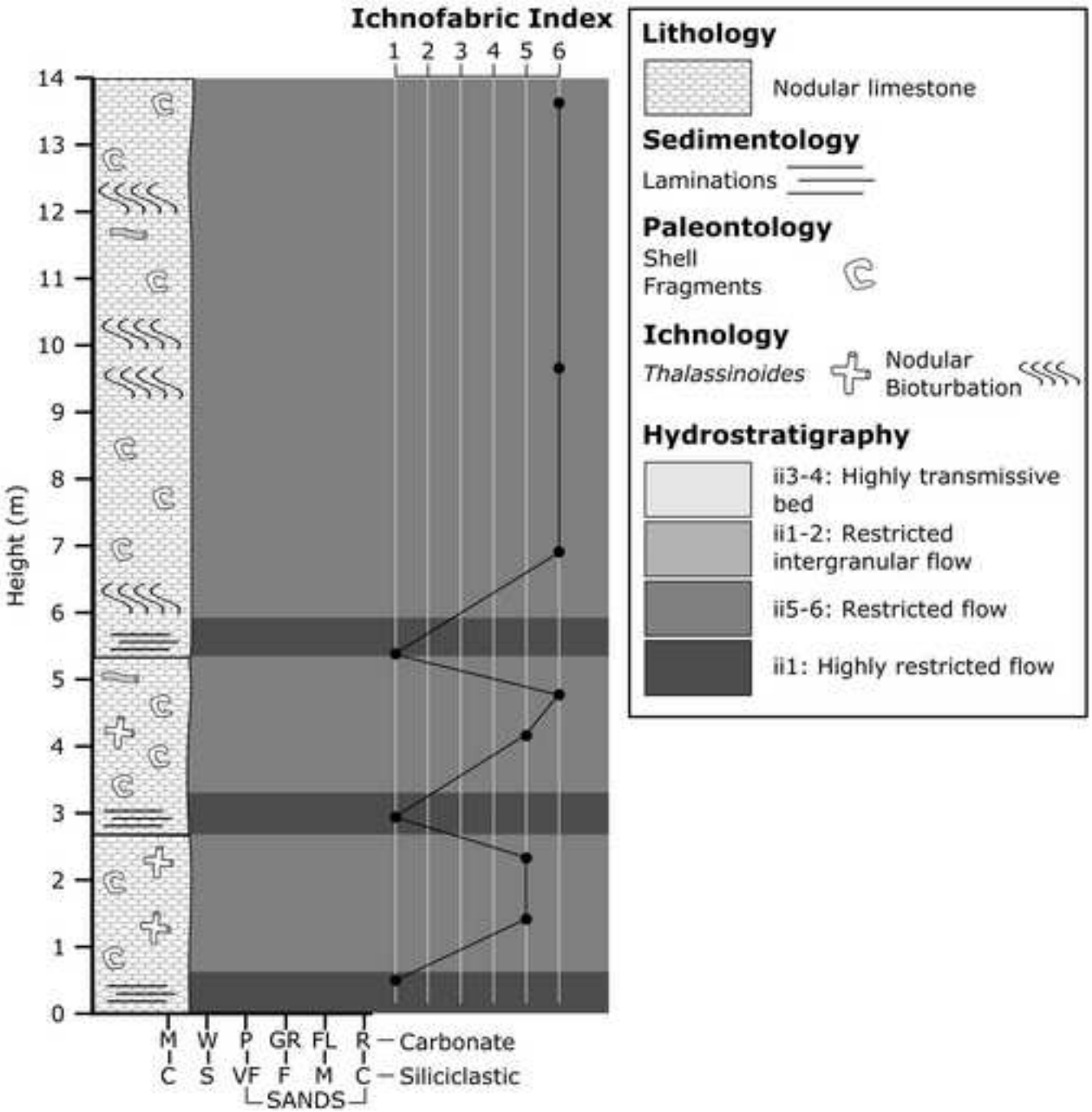
Ichnofabric Index
1 2 3 4 5 6
Height (m)
0 1 2 3 4 5 6 7 8 9 10 11 12 13 14
M W P GR FL R — Carbonate
C S VF F M C — Siliciclastic
SANDS
Lithology
Nodular limestone
Sedimentology
Laminations
Paleontology
Shell Fragments
Ichnology
Thalassinoides
Nodular Bioturbation
Hydrostratigraphy
ii3-4: Highly transmissive bed
ii1-2: Restricted intergranular flow
ii5-6: Restricted flow
ii1: Highly restricted flow

Figure 11

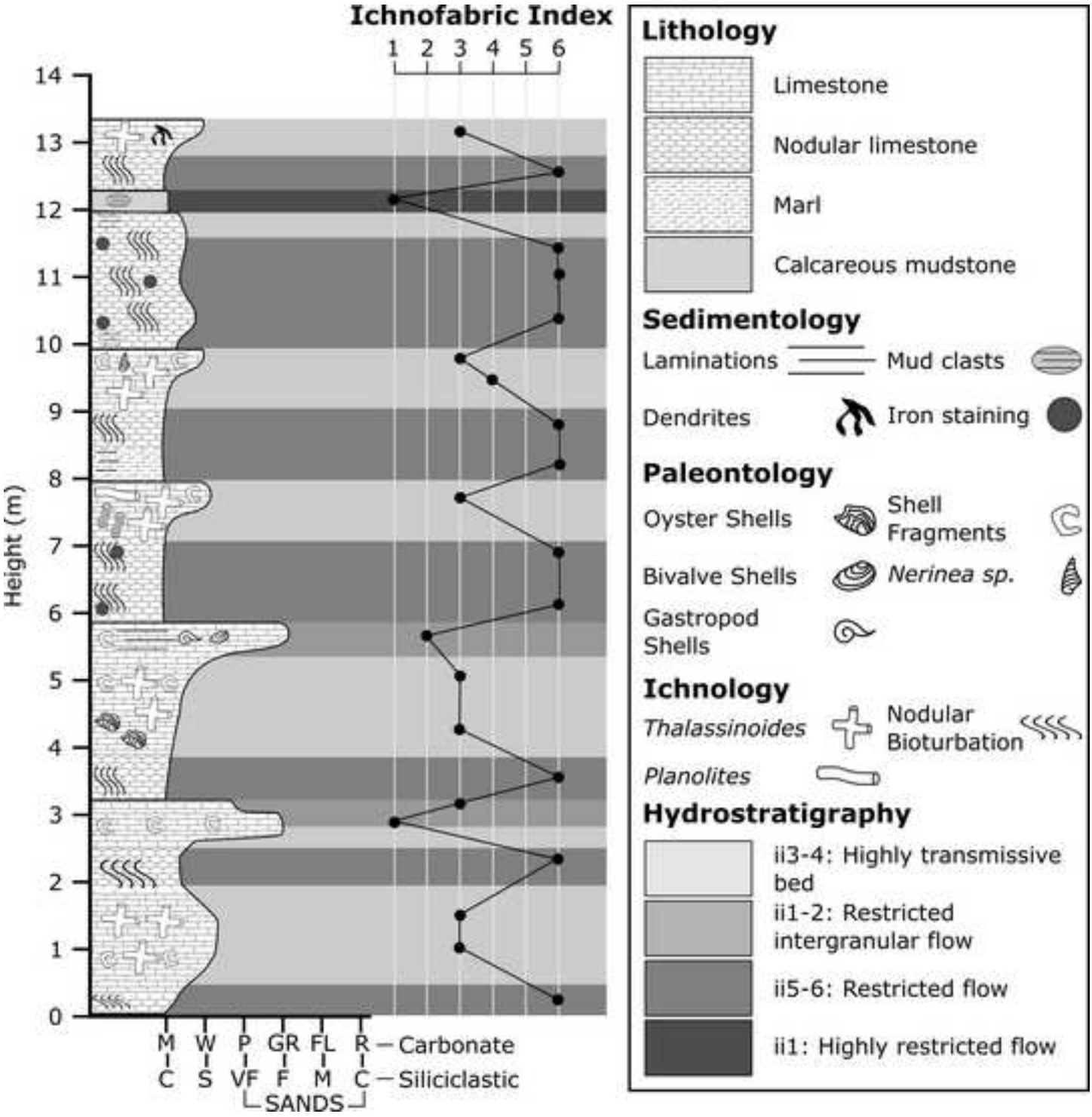
Ichnofabric Index
1 2 3 4 5 6
Height (m)
0 1 2 3 4 5 6 7 8 9 10 11 12 13 14
M W P GR FL R — Carbonate
C S VF F M C — Siliciclastic
SANDS
Lithology
Limestone
Nodular limestone
Marl
Calcareous mudstone
Sedimentology
Laminations
Mud clasts
Dendrites
Iron staining
Paleontology
Oyster Shells
Shell Fragments
Bivalve Shells
Nerinea sp.
Gastropod Shells
Ichnology
Thalassinoides
Nodular Bioturbation
Planolites
Hydrostratigraphy
ii3-4: Highly transmissive bed
ii1-2: Restricted intergranular flow
ii5-6: Restricted flow
ii1: Highly restricted flow

Figure 12

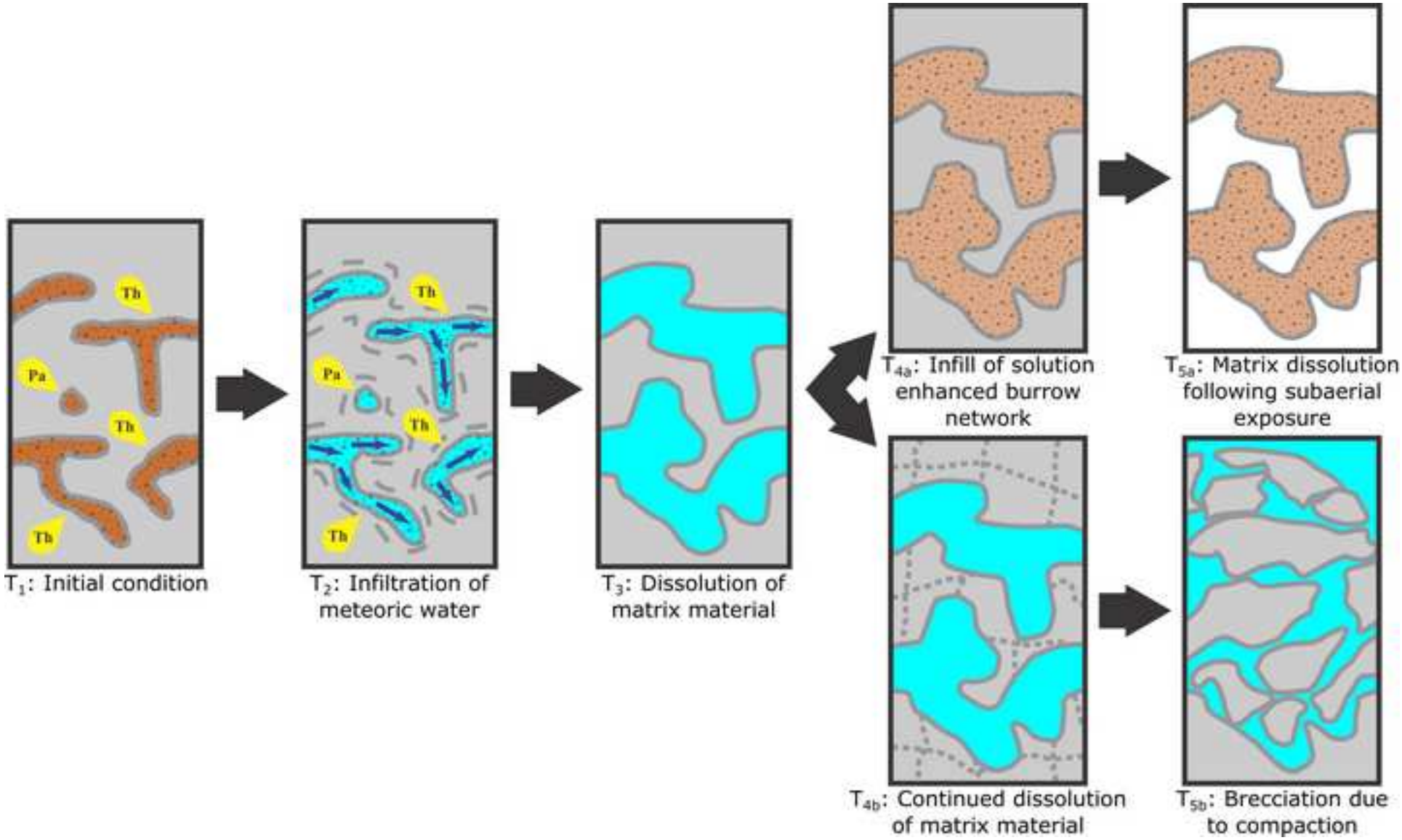
Th
Pa
Th
Th
T_1: Initial condition
Th
Pa
Th
Th
T_2: Infiltration of meteoric water
T_3: Dissolution of matrix material
T_{4a}: Infill of solution enhanced burrow network
T_{5a}: Matrix dissolution following subaerial exposure
T_{4b}: Continued dissolution of matrix material
T_{5b}: Brecciation due to compaction